Whole-Sequence Rear-End Impact Simulations with an Active Human Body Model

Jonas Östh, Katarina Bohman, Lotta Jakobsson

Abstract Rear-end crashes involve car occupants of varying size, seating position, and pre-crash conditions, all of which could influence the risk of whiplash injury. This study utilised an average male active Human Body Model (HBM) in a whole-sequence rear-end impact scenario. The HBM was positioned in a finite element model including a seat, floor, steering wheel and seat belt, and a scenario consisting of braking followed by a ΔV 16 km/h rear-end impact was simulated. An intervention in the form of 200 N Electrical Reversible Retraction (ERR) was studied, as well as variations of the muscle activation conditions. Braking had a considerable effect on driver head-neck kinematics in the crash phase because it increased the backset, while the simulated ERR intervention mitigated some of the backset increase. Muscle activations generated during the braking influenced intervertebral segment rotations and spine lengthening during the crash phase. This study demonstrated that utilising an active HBM in whole-sequence rear-end impact scenarios allows for investigation of muscle activation effects and pre-crash interventions for a car driver. Further leveraging HBM morphing capabilities could lead the way to assessing the whole population of occupants and scenarios with varying size, shape, and sitting posture, in both driver and passenger occupant positions.

Keywords rear-end impacts, whiplash injuries, occupant posture, human body model, active muscle

I. INTRODUCTION

Low severity cervical spine injuries, while posing a low threat to life, are among the most significant types of injury sustained in car crashes due to their frequency and the long-term impairments they cause [1–2]. These injuries, commonly referred to as whiplash injuries, encompass a broad range of symptoms and are likely caused by multiple injury mechanisms, making prediction and prevention challenging. Whiplash injuries can occur in all types of crash, with rear-end impacts remaining a frequent cause.

Efforts to address whiplash injuries began in the 1970s with the introduction of head restraints, which were proven effective in preventing neck hyperextension in rear-end impacts. In the late 1990s, Saab and Volvo introduced whiplash-protection seats, which were shown to be effective in preventing whiplash injuries [3–4]. These innovations led to the development of standardised tests in the early 2000s by organisations such as the Insurance Institute for Highway Safety (IIHS) and Euro NCAP, to evaluate and rate the ability of seats and head restraints to prevent whiplash injuries. However, a recent study by the IIHS found that despite most modern seats receiving good ratings, there is still a wide range of injury claim rates in insurance data [5]. This suggests that some risk factors are not being fully addressed. The IIHS [5] evaluated whether three different rear-impact crash pulses (ΔV of 16 km/h, 20 km/h, and 24 km/h) and associated test metrics improved correlations with injury claim rates for modern seats. They discovered that the higher crash pulse (ΔV 24 km/h) was the best predictor of injury claims. Besides impact characteristics, several other factors have been shown to influence risk of whiplash injuries in rear-end impacts, such as individual differences in size, age, sex, sitting postures at time of impact, and seat position in the car [6–9].

With the purpose of representing human-like occupant responses, including torso-straightening motion in rear-end impact crash tests, the Anthropomorphic Test Device (ATD) BioRID was developed as a Swedish joint venture during the 1990s [10]. A mathematical counterpart was developed early [11], and several versions of BioRID models have followed. As a complement to the mid-sized male BioRID Finite Element (FE) model, the European project ADSEAT developed a mid-sized female Finite Element (FE) model counterpart, called EvaRID

J. Östh, PhD, (e-mail: jonas.osth@volvocars.com, tel: +46 728 88 91 72) and K. Bohman, PhD, are Technical Experts, and L. Jakobsson, PhD, is a Senior Technical Leader at the Volvo Cars Safety Centre, Gothenburg, Sweden. L. Jakobsson is an Adjunct Professor and J. Östh is an Adjunct Associate Professor at Chalmers University of Technology, Gothenburg, Sweden. All authors are associated with SAFER – Vehicle and Traffic Safety Centre at Chalmers, Gothenburg, Sweden.

[12]. Two physical Seat Evaluation Tools, representing a mid-sized female and male, have also been created to enable assessment and validation of seat models prior to virtual evaluation [13] that could encompass varying occupant size and sex, for instance by using Human Body Models (HBMs) and parametric morphing [14–15].

In a previous study [16], an FE model of the BioRID was shown to be able to also represent car passenger kinematics resulting from braking. It was subsequently used for whole-sequence assessment of rear-end impacts preceded by a braking intervention, an event that will influence the distance between the head and head restraint at the start of impact (the backset). Including a countermeasure to the forward motion induced by braking in the form of an Electrical Reversible Retractor (ERR) seat-belt reduced the backset at the start of the crash and reduced relative head–T1 kinematics.

While it was found that the BioRID could have application in whole-sequence rear-end impact scenarios [16], HBMs with active musculature have been used more extensively for other whole-sequence scenarios. Previous studies, for example, have studied effect of braking in combination with frontal impact [17–20], side impact [20–23], and rear-end impact [24], showing that the change in occupant initial posture affects the kinematics during crash [20], and also that the simulated muscle activations have the potential to affect injury predictions from the HBM [17,24]. Another capability of active HBMs compared to the BioRID is the ability to simulate driver interaction with the steering wheel through the arms [25], while tests with the BioRID are typically conducted with the arms in the lap, representing a car passenger rather than a driver.

To enable simulation of human muscle responses, HBMs such as the SAFER HBM [14] have been equipped with muscle elements and control algorithms that aim to reproduce active human muscle responses under both vehicle manoeuvres and crash conditions. Some early studies, focusing on cervical spine kinematics and injury tolerance levels, utilised optimisation to find activation levels that could stabilise the head and neck under gravity as well as represent an initially tensed state [26], while others have used experimental recorded muscle activations and applied those to simulation models [27–28]. For vehicle manoeuvre events, several studies have implemented feedback control to generate muscle activations and to validate the against kinematics recorded from volunteer experiments [19, 29–30]. Some work has utilised HBMs with muscle activation to study neck responses in rear-end impact, focusing on the muscle effect in the crash-phase [24, 31–32] which is easily motivated as the human cervical spine requires muscle stabilisation to maintain an upright seated posture. Several studies focusing on cervical spine injury tolerance has concluded that muscle activation is an important factor for both high [26] and low severity injuries [33].

Present standardised whiplash injury assessment tests with the BioRID provide limited insights into real-world whiplash injury protection need. They are limited because the reflect the seat and head restraint performance only, and do not take into account the car design, other restraints, the pre-crash situation, occupant posture or driver or passenger position. As was shown in a previous study, whole-sequence events could be studied for car passengers to some extent with the BioRID [16], but other factors, such as the influence of a variation of occupant size, shape, posture or driver or passenger position, would not be possible with current ATD based methods. Active HBMs could offer this ability to some extent as they can be adjusted by parametric morphing to account for size and sex effects [14, 15], and can represent both occupant and driver vehicle manoeuvre muscle responses.

The present study aims to investigate the influence of braking, interventions during the braking in the form of an ERR, and the effect of muscle control strategies on the head-neck kinematics in rear-end impacts. An overarching aim is to contribute to understanding of important factors for simulating whole-sequence rear-end impacts with active HBMs.

II. METHODS

Whole-sequence rear-end impact simulations were conducted with the SAFER HBM v11 50th percentile male (M50) [34]. The HBM was positioned in a sled with a simulation FE model of a Volvo WHIPS generation 2 front seat [35], previously used for whole-sequence simulations with the BioRID ATD [16]. To represent a driver environment, the sled simulation model was complemented with a steering wheel, Fig. 1.

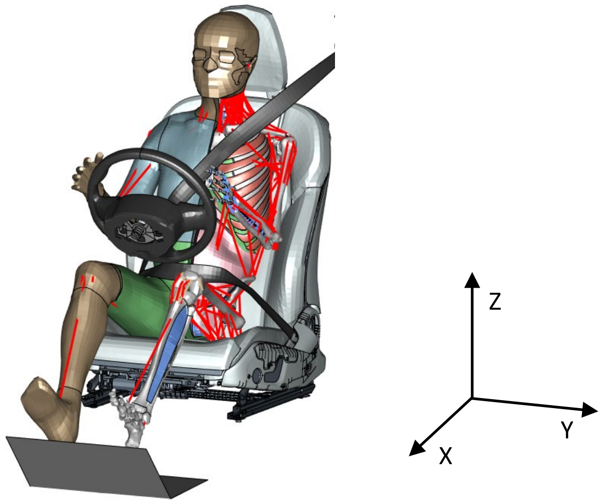

Fig. 1. The SAFER HBM v11 M50 model in the whole-sequence rear-end impact simulation FE model.

Human Body Models

The SAFER HBM v11 M50 (Fig. 1) has a stature of 1.75 m and a mass of 77 kg, as reported for M50 subjects [36], and a body shape representative of a 45-year-old. Notable features of the SAFER HBM are a detailed rib cage with strain-based injury prediction [37] and the KTH head model [38]. For v11 [34], several updates were made, such as refined detailed pelvis model with population average M50 shape [39] and new lumbar [40] and cervicothoracic spine, including updated costovertebral joints, new shoulder girdle bones and femora, as well as updated lower extremity soft tissues [34]. For whole-sequence simulations, the SAFER HBM utilises Angular Position Feedback (APF) control [41], which generates muscle activations proportional to relative motions of the trunk and head in the pre-crash phase. For v11, some cervical spine muscles (trapezius, levator scapulae, splenius capitis, splenius cervicis and parts of erector spinae longissimus) were rerouted via points in the neck soft tissues and some lumbar dorsal muscles (parts of erector spinae longissimus) were rerouted via the ribcage using the LS-DYNA keyword *PART_AVERAGED to better capture their line of action [34].

The controller settings, including the Proportional – Integral – Derivative (PID) gains, were not modified. For the present study, the baseline APF control was set to be active during the pre-crash phase and then muscle activations were held constant for the subsequent crash phase [17, 23].

Moreover, for the present study the updated SAFER HBM v11 M50 was validated for driver autonomous brake intervention kinematics using a simulation setup previously used to validate passenger HBM responses [41] complemented with a steering wheel for the present study to represent a driver environment. Validation results for the updated SAFER HBM v11 are included in Appendix A. The validation is representative of the braking part of the whole-sequence scenario outlined in the next section but does not include the rear-end impact part of it.

Whole-Sequence Rear-End Impact Scenario

For the present study, a whole-sequence rear-end scenario was created consisting of a braking event followed by a rear-end impact. Such as scenario could be caused by a harsh braking host vehicle, impacted by a following vehicle with an inattentive driver driving too close, not braking hard enough or being sleepy [42].

The first part of the scenario, Fig. 2, was 300 ms to allow for APF controller initialisation and settling of the HBM under gravity. During the positioning phase, the feet and hands of the HBM were positioned to the footrests and steering wheel using positioning cables, and a seat squash between the HBM and seat was carried out. After positioning, the cables for the feet were removed and for the hands they were locked at zero-length, creating a moment free connection between the hands and the steering wheel. Then a braking acceleration was ramped up to 11 m/s^2 over 200 ms and held for another 460 ms, giving braking ΔV of 22 km/h. These parameters were selected using engineering judgment and would represent a harsh autonomous braking intervention, for instance in a rapid queue onset situation, followed by a rear-end impact in the form of the IIHS ΔV 16 km/h rear-end impact pulse [43], Fig. 2.

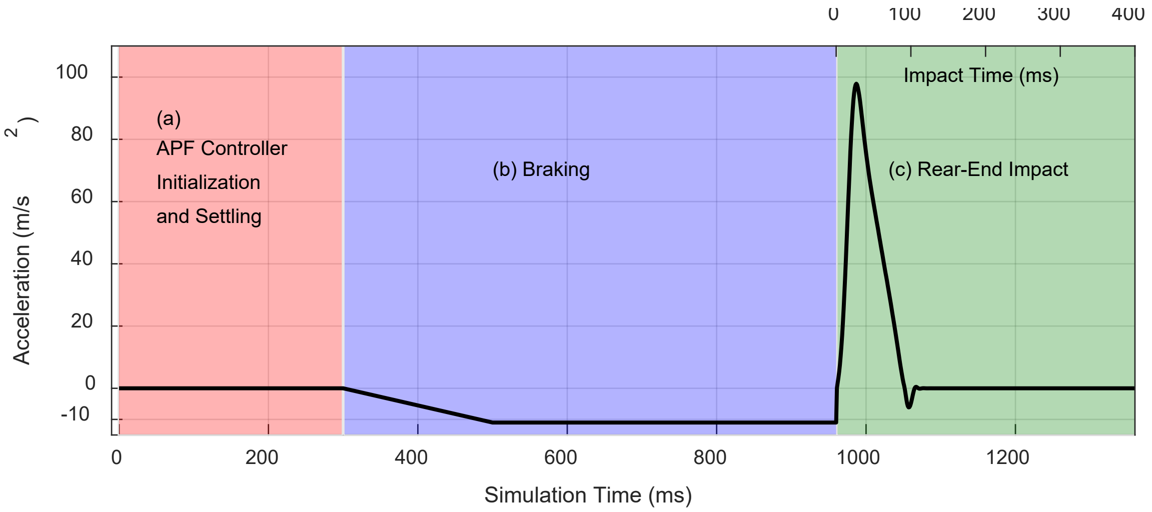

Fig. 2. Whole-sequence rear-end impact scenario: (a) 300 ms controller initialisation and settling of the HBM under gravity.; (b) 660 ms braking intervention with a ΔV of 22 km/h; (c) 400 ms rear-end impact with a 16 km/h ΔV.

Simulations

The first simulation, Sim. 1 (see Table I), was run with only the initialisation and crash phase to create a baseline response for comparing the effect of braking included in the whole-sequence scenario. Two seat-belt variations were modelled, one with a regular retractor, that was locked throughout the entire scenario (all simulations), and one with a nominal 200 N ERR tension added at the start of the braking part of the scenario (Sim. 3). The ERR tension was then maintained for the full braking and rear-end impact phase of the simulation. In addition to the belt variation, muscle control variations were made to investigate the effect of the muscle control on the HBM responses. For Sim. 4 the APF muscle control was turned off at the start of the rear-end impact crash-phase, to show the model in-crash and rebound responses without muscle forces and with the same initial conditions as for Sim. 1. For Sim. 5 the HBM muscle control was switched off and only the crash phase was simulated, without the initialisation and settling, with the HBMs starting in a higher and more rearward position (Table II). Sim. 1 to Sim. 3 were also repeated with hands positioned in the lap instead of on the steering wheel and without active arms to demonstrate simulation of a passenger compared with a driver occupant (Appendix D). The simulations were run using LS-DYNA R12.2.2 MPP Single Precision (ANSYS/LST, Livermore, CA).

TABLE I
SIMULATION MATRIX.

Sim.	**Muscle Control**	**Belt**	**Initialisation (ms)**	**Braking (ms)**	**Rear-end Impact (ms)**	**Total Simulation Time (ms)**
1	Active	No ERR	300	0	400	700
2	Active	No ERR	300	660	400	1360
3	Active	200 N ERR	300	660	400	1360
4	Switch Off	No ERR	300	0	400	700
5	Passive	No ERR	0	0	400	400

Analysis

The HBM cervical spine responses were analysed at three levels. First, spinal kinematics and backset (head-to-head restraint distance calculated as the minimum distance between the head and head restraint surfaces) was recorded and Head–T1 relative acceleration and velocity in the X-direction, capturing the overall head-neck kinematics. As a measure of the rebound out of the seat, the T1 velocity at the time the head left the head restraint was recorded. Second, the dynamic length of the cervical spine was analysed using markers attached to the centre of the spinal canal for each vertebra from C1 to T1, Fig. 3. The length of the spinal canal was calculated as the sum of the Euclidean distance between the C1–T1 vertebra markers. The initial spinal length (C1–T1) of the SAFER HBM v11 M50 is 118 mm. Third, dynamic intervertebral rotations were analysed as the difference in Y-rotation for the spinal canal markers for each segment from C2 to T1 during the time the head was in contact with the head restraint. For these angles an increase in angle means flexion of the segment, while a decrease means extension. The post-processing was carried out using Meta v 24.1.3 (BETA CAE Systems, Luzern, Switzerland) and Matlab 2019b (Mathworks, Nattick, MA, USA). Image time series of the braking in Sim. 1 and Sim. 2, and of the rear-end impact in Sims. 1–5 are shown in Appendix C, Fig. C2 and Fig. C3. The spinal trajectory data is presented in a coordinate system with origin in the left from bolt for the seat.

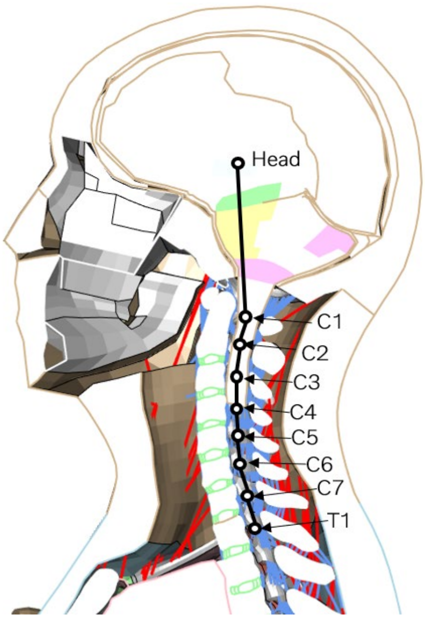

Fig. 3. HBM head and neck sagittal plane cross-section, showing the location of head centre of gravity and the spinal canal vertebral markers used for spine kinematics analysis.

III. RESULTS

During the initialisation phase in Sim. 1–4 the HBM moved down substantially (58 mm for the head Centre of Gravity (CoG)) but was able to stabilise the posture at a position 6 mm more forward for the head CoG position after settling. Of this downward movement 34 mm was due to the HBM-seat interaction. This forward motion during the initialisation phase led to a marginally higher backset of 23 mm at the start of the rear-impact, compared with 12 mm before the settling, Table II. In addition to the more forward position, the spinal curvature after settling became more lordotic, Fig. C1 in Appendix C and a minor amount of slack was created in the seat-belt routing.

TABLE II

SUMMARY OF INITIAL GEOMETRY AND PEAK KINEMATIC RESPONSES. ACC. = ACCELERATION. VEL. = VELOCITY.

	Backset (mm)			Head-Head Restraint Interaction during Impact Time		Min Head–T1 X acc. (g)	Max Head–T1 X acc. (g)	Min Head–T1 X vel. (m/s)	Spinal Canal Length (mm)		Peak Intervertebral Flexion (+)		Peak Intervertebral Extension (-)	
Sim.	Initial	After Settling	At Start of Impact	Contact (ms)	Rebound (ms)				At Start of Impact	Peak	Level	(°)	Level	(°)
1	12	23	23	48	145	-3.7	5.6	-0.5	111	129	C6C7	6.1	C2C3	-4.3
2	12	23	159	83	155	-9.3	16.2	-2.7	113	113	C2C3	0.4	C6C7	-3.1
3	12	23	95	70	145	-12.1	15.4	-2.8	114	121	C3C4	2.2	C7T1	-6.2
4	12	23	23	48	148	-4.6	4.2	-0.4	111	128	C6C7	7.7	C3C4	-7.1
5	12	N/A	12	45	162	-3.3	5.0	-0.5	118	129	C7T1	7	C3C4	-5.6

Effect of Braking

The braking led to a substantial increase in backset to 159 mm in Sim. 2., Table II, Fig. 4 and Fig. 5. In addition to the distinct difference in initial position and backset, it is worth noting the large difference in the rebound kinematics for which the head moves 50 mm less forward, and considerably less downward. The braking simulations also had considerably larger extensor muscle activation in the neck, trunk, and arms (Table BI in Appendix B), as a result of the braking because the muscle activations in the HBM were retained from the pre-crash phase to the crash phase.

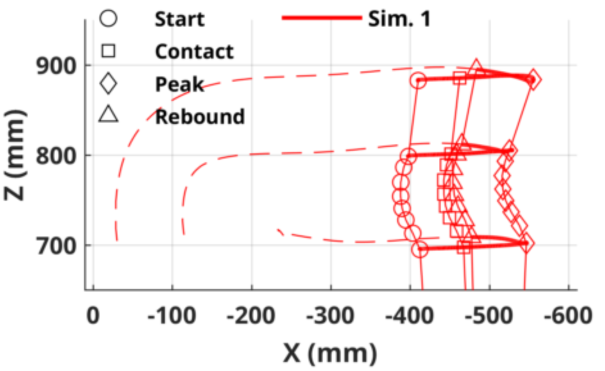

Fig. 4. The HBM spinal kinematics in Sim. 1 during the rear-end impact. The upper most marker is the head CoG, the lower most in the centre of the spinal canal of T1. The thick solid trajectories show the loading phase, and the thin dashed show the rebound trajectories.

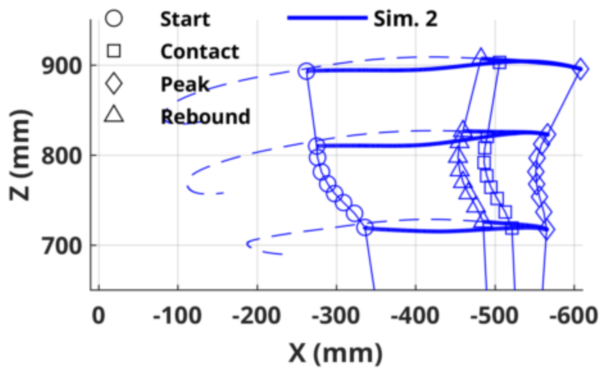

Fig. 5. The HBM spinal kinematics in Sim. 2 during the rear-end impact. The upper most marker is the head CoG, the lower most in the centre of the spinal canal of T1. The thick solid trajectories show the loading phase, and the thin dashed show the rebound trajectories.

The forward motion during the braking in Sim. 2 led to a later head contact timing, at 83 ms compared with 48 ms in Sim. 1 without the braking, Fig. 6 and Table II. While the peak T1 x-acceleration only varied about 2 g between these two simulations, the peak head x-acceleration was considerably higher for Sim. 2, also giving higher peak relative Head–T1 acceleration and velocity, e.g. −3.7 g compared with −9.3 g for Sim. 1 and Sim. 2, respectively.

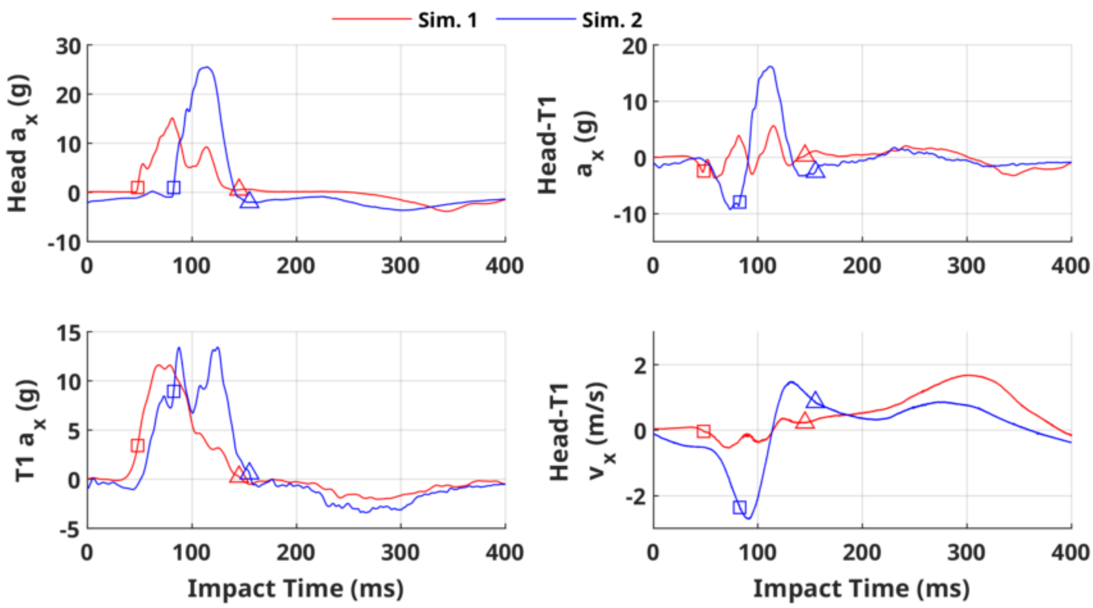

Fig. 6. The HBM head–T1 rear-end impact kinematics in Sim. 1 and Sim. 2. The square marker indicates the head-to-head restraint contact time, and the triangle timing of rebound when the head left the head-restraint.

The length of the cervical spine was only marginally affected by the initial impact phase, Fig. 7, with length increases in the order of 1 mm for both Sim. 1 and Sim. 2. In the rebound phase, after leaving the contact with the head restraint, the active HBM without braking in Sim. 1 had an increased cervical spine length of 18 mm compared to at the start of the crash phase. For Sim. 2, with the braking that gave increased cervical extensor muscle activations (Table BI in the Appendix) and the extension of the spine was close to 0 mm also during the rebound phase.

While there was only a minor change in spinal length during the head-to-head restraint contact phase, there were notable changes in intervertebral segment rotations, Fig. 8. For the baseline Sim. 1 without braking, the lower segments moved in flexion for the active HBM, with a peak motion at C6C7 of 6.1°, Table II. For the simulations with braking, Sim. 2 and Sim. 3, there was flexion of the upper segments instead and extension of the lower segments for the HBM. During rebound, all segments move into flexion except for Sim. 2, which had a low level of intervertebral flexion during the rebound phase.

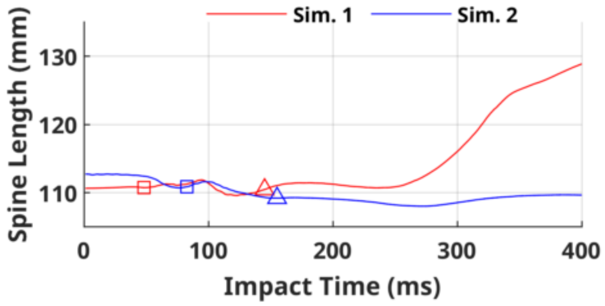

Fig. 7. The HBM cervical spine length during the rear-end impact for Sim. 1 and Sim. 2, calculated as the Euclidean distance between the C1–T1 vertebra markers (see also Fig. 3). The square marker indicates the head-to-head restraint contact time, and the triangle timing of rebound when the head left the head-restraint.

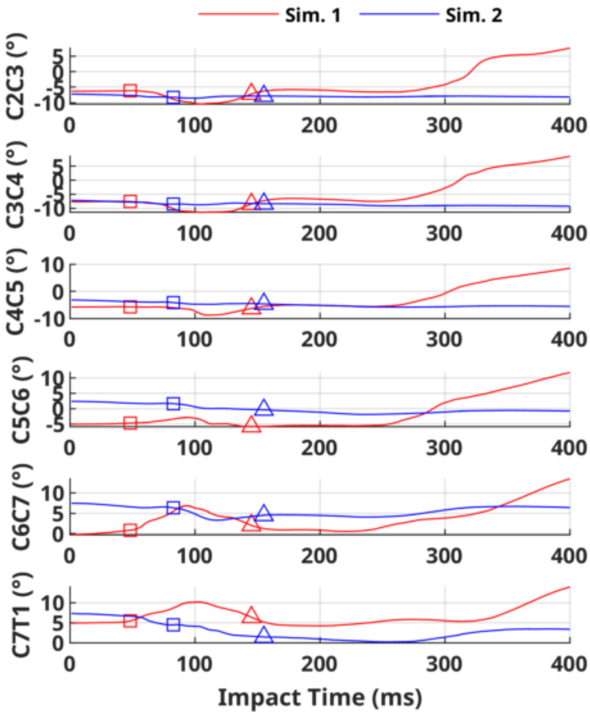

Fig. 8. The HBM cervical spine segment rotations during the rear-end impact in Sim. 1 and Sim. 2. The square marker indicates the head-to-head restraint contact time, and the triangle timing of rebound when the head left the head-restraint.

Effect of ERR

The addition of the ERR during the braking for Sim. 3 led to a reduction of the forward motion and the initial backset at the start of the crash phase was 95 mm. This led to a head-to-head restraint contact at 70 ms, half-way in between that of Sim. 1 and Sim. 2. In addition, the peak head x-acceleration was reduced as a consequence of the smaller backset, from 25 g in Sim. 2 to 21 g in Sim 3., Fig. 6. However, due to earlier contact with the torso and thereby earlier T1 peak acceleration, the peak negative Head–T1 acceleration was higher for Sim. 3 compared with Sim. 2. The rebound velocity out of the seat for the torso was reduced from 2.9 m/s for Sim. 2 with braking to 2.4 m/s for Sim. 3 with the ERR during braking. A comparison of the spinal kinematics between Sim. 2 and Sim. 3 is shown in Fig. 10.

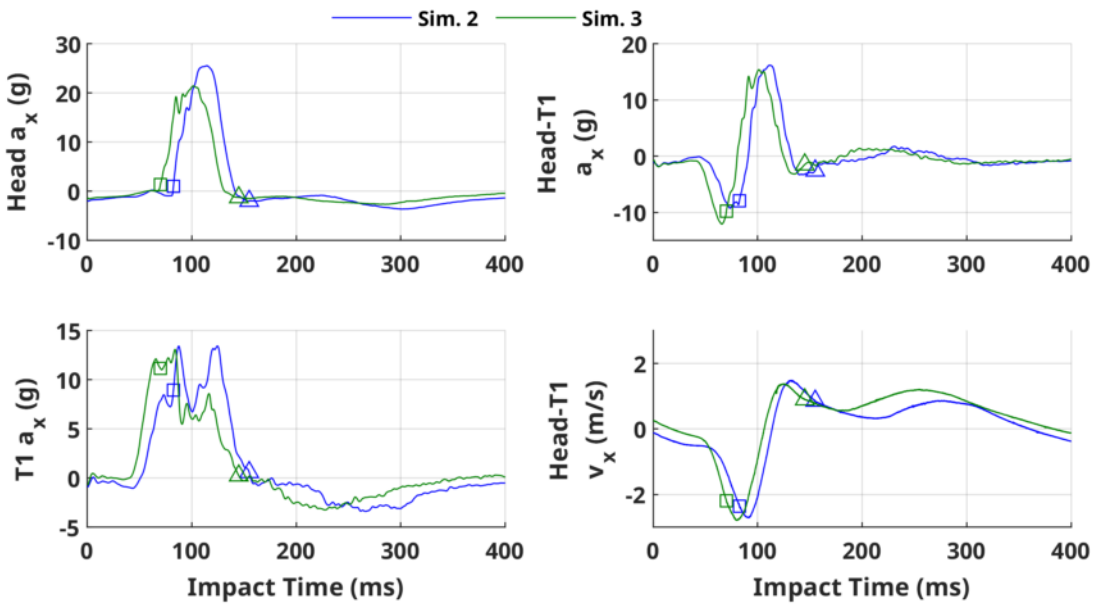

Fig. 9. The HBM head-T1 kinematics during the rear-end impact in Sim. 2 and Sim. 3. The square marker indicates the head-to-head restraint contact time, and the triangle indicates the timing of rebound when the head left the head-restraint.

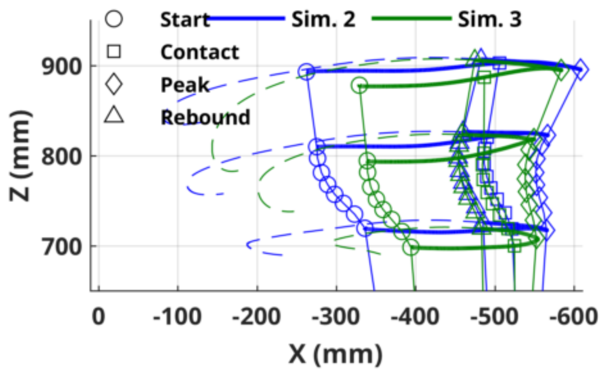

Fig. 10. The HBM spinal kinematics during the rear-end impact with braking without ERR, Sim. 2, and with ERR, Sim. 3. The upper most marker is the head CoG, the lower most in the centre of the spinal canal of T1. The thick solid trajectories show the loading phase, and the thin dashed show the rebound trajectories.

Effect of Muscle Control

The simulation for which the muscle control was turned off at the start of the crash phase, Sim. 4, had a somewhat more upward motion than the active models in Sim. 1 and Sim. 2, Fig. 4 and Fig. 5. This was likely due to some elastic spring-back in the cervical spine as the muscle contractions were released. The passive HBM, Sim. 5, moved downwards during the crash phase and continued a downward trajectory during the rebound phase, Fig. 11, while the simulations with the active HBMs after settling moved slightly upwards during the crash phase, Fig. 4 and Fig. 5.

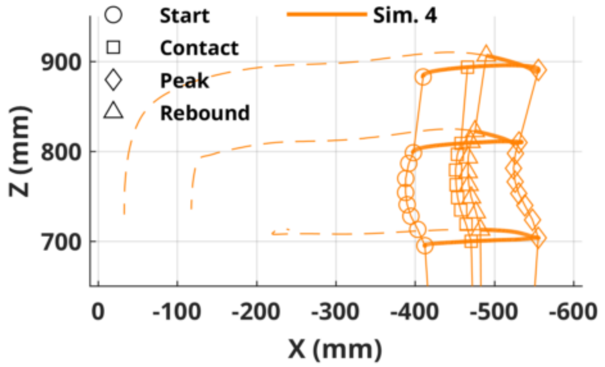

Fig. 10. The HBM spinal kinematics during the rear-end impact in Sim. 4. The upper most marker is the head CoG, the lower most in the centre of the spinal canal of T1. The thick solid trajectories show the loading phase, and the thin dashed show the rebound trajectories.

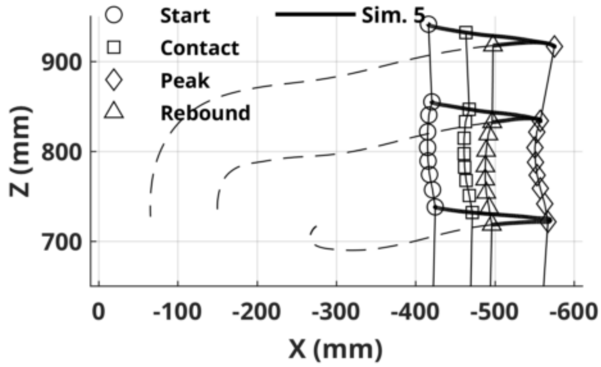

Fig. 11. The HBM spinal kinematics during the rear-end impact in Sim. 5. The upper most marker is the head CoG, the lower most in the centre of the spinal canal of T1. The thick solid trajectories show the loading phase, and the thin dashed show the rebound trajectories.

Compared with the baseline Sim. 1 with constant muscle activation during the crash and rebound phase, the crash response was similar for the head, T1 and Head–T1 relative kinematics for the Sim. 4 that had the same initial position at the start of the crash phase. The passive HBM in Sim. 5, which started higher up with a somewhat lower backset, had marginally lower peak head and T1 x accelerations, Fig. 12.

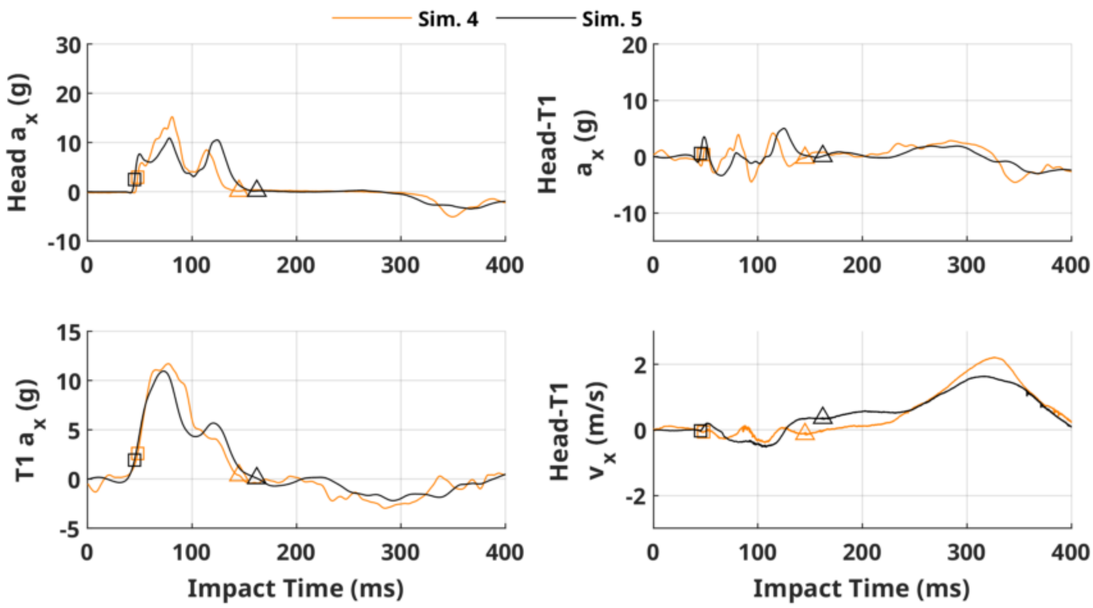

Fig. 12. The HBM head-T1 kinematics during the rear-end impact in Sim. 4 and Sim. 5. The square marker indicates the head-to-head restraint contact time, and the triangle indicates the timing of rebound when the head left the head-restraint.

IV. DISCUSSION

This study investigated the whole-sequence rear-end impact response of an active HBM modelling a driver, subjected to a braking event followed by a ΔV 16 km/h rear-end impact. As the SAFER HBM M50 v11 has an updated spine and muscle routings for the neck [34], it was first validated with respect to its braking kinematics (Appendix A). The validation showed that the forward head and T1 displacements were on the upper end of the volunteer corridors, in line with previous versions of the model [25]. This means that the predictions of the HBM in the whole-sequence rear-end impacts are conservative in that they predict motions away from the head restraint, which are on the high side, during the initial braking event.

The major effect of the braking in the simulations was the increased backset at the start of the crash phase. Without braking, the backset was 23 mm after settling of the HBM, and with the braking it was 159 mm, a difference likely large enough to have an influence on the injury outcome. This was also evident in the current simulations where this larger backset led to an increase in Head–T1 relative acceleration and velocity, which has been suggested to correlate with the risk of whiplash injury [44]. One study [45], which derived the Neck Injury Criterion (NIC) suggested that the elongation of the spine during the S-shaped motion in a rear-end impact would contribute to a pressure gradient that could injure the spinal ganglia, which could be the cause of whiplash injury. In the present study the length of the spinal canal was monitored, and it was found that it did not change much during the initial part of the impact for any simulation. For a repeated simulation with deactivation of the muscles at the start of impact in Sim. 2 (Appendix E), the spine did lengthen during the impact, which is why this effect was due to the muscle contractions constraining the head.

While the length of the spinal canal did not change during impact due to the muscle contractions, the intervertebral segment rotations were affected by the presence of braking or not. For the baseline simulation, Sim. 1, the lower cervical segments from C5C6 to C7T1 moved in flexion during the crash, with up to 6° rotation over 50 ms. For the simulation with braking, the lower segments showed extension of lower magnitude, most likely due to the cervical spine extensor activation and that the spine had moved in flexion due to the braking. Differences in spinal rotation, the so-called S-shape, have been reported in testing with both volunteers [46] and PMHS [47] and are also suggested to contribute to the risk of whiplash injury.

The ERR countermeasure during the braking phase in Sim. 3 was successful in reducing the forward displacements of the head and torso, similar to the previous study with the BioRID ATD [16]. In the present study with the HBM the positive relative Head–T1 acceleration peak during impact was reduced with the ERR, but the initial negative relative acceleration peak was somewhat higher. In addition to a reduced backset and earlier head contact time, the ERR led to reduced deflection of the seat, Fig. 10 , in the subsequent rear-end impact. This also reduced the subsequent forward rebound displacement. While the BioRID [16] showed an unanimous improvement in the relative Head–T1 acceleration with decreased backset, the HBM's higher negative peak acceleration indicates more relative movement with the ERR even though the backset was reduced. This indicates that for an HBM that more closely resembles the human anatomy more factors than the backset were influential to this result, most likely the muscle contraction level, which also varied between the simulations.

Another factor that was different in the present study compared with the previous [16] was the inclusion of active arms that interacted with the steering wheel. The hand–to–steering wheel contact was modelled as a moment free joint. During the impact phase, tensile forces in the steering column of 820–1200 N were recorded depending on the muscle contraction state, giving additional constraint of the torso through the arms.

In Sims 1–5, three different muscle contraction conditions were simulated. For Sims 1–3, the APF controllers were active during the initialisation phase and the braking phase. The muscle activations were then fixed at their value at the start of the crash-phase, Table BI in Appendix B. The muscle activations affected the elongation of the spine during the rebound phase. For the simulations with the braking, Sim. 2 and Sim. 3, there was higher muscle activations and no elongation of the spine during the rebound phase while for the baseline, Sim. 1, there was a peak elongation of 18 mm. While the HBM muscle activations were extrapolated from the braking or initialisation phase, this demonstrates that occupant cervical spine muscle activations could have a considerable effect on the rebound kinematics, which has been suggested as one possible cause of whiplash injury [48] in a rear-end impact. In the present study, the torso T1 velocity out of the seat was increased due to the braking and then reduced by the introduction of the ERR during the braking.

The muscle activation levels of car drivers and occupants subject to braking interventions are difficult to validate, but some efforts have been made for previous versions of the SAFER HBM [41]. Overall, the APF controller is biofidelic by generating low magnitude activation levels to maintain the upright posture when the model is not perturbed, and high activation levels during braking. Both these conditions should be relevant to study for a sub-sequent rear-end impact. The assumption that the muscle activation levels remain constant during the crash phase is an extrapolation. Previous research has shown that cervical spine muscle reaction in low level rear-end impact can occur from 50 ms after the onset of the impact pulse [50–52], which overlaps with the peak negative relative Head–T1 x acceleration observed in the present study (around 60–75 ms) to after the head has left the contact with the head restraint and started the rebound motion (145–162 ms). Simulations incorporating a startle response [17] for 100 ms, starting 50 ms into the impact phase, were also tried, but did not provide any visible alteration of the crash phase head neck response of the HBM and were therefore omitted from the paper. When the muscle controllers were turned off, Sim. 4, during the crash phase only marginal differences were seen in comparison with the posture maintaining contractions in Sim. 1 when the same initial position of the HBM was used. When the passive HBM was simulated without the settling phase, some more variation in response was observed, likely due to a slightly higher and closer position relative to the seat back and head restraint.

Challenges of Active HBM Whole-Sequence Rear-End Impact Simulations

In the present study, an active M50 HBM was used to study whole sequence rear-end impact simulations. In contrast to using BioRID [16], the use of a HBM enables the inclusion of the effect of active musculature and representation also of a driver which could be less affected by pre-crash braking than a passenger due to the steering wheel constraint (see comparison between predicted driver and passenger response by the HBM in Appendix D). This opens the way for a variety of other whole-sequence scenarios that have been simulated with active HBMs, such as evasive steering manoeuvres [17]. The posture maintaining muscle activations that were generated by the APF controller, Table BI in Appendix B, were of the same magnitude as reported for volunteers during regular driving [49]. Therefore, by using the active HBM instead of an ATD or a passive HBM, an occupant driver model that is in semi-equilibrium with gravity using representations of the muscles can be simulated and the present study demonstrates this.

The use of a HBM will also allow for study of an expanded population, beyond the average male, using the ability of FE HBMs to be morphed to create a wide range of occupants of varying size [15] and also to account for sex effects [14]. For the present study, an attempt was made also run simulations with a morphed F50 model, using parametric morphing [15] and scaling of muscle cross-sectional areas as described in [14]. For this F50 model, the settling phase led to an initial posture with a backset of 112 mm and an S-shaped cervical spine that was considered unphysiological. Hence, no results from this model were included in the paper. This attempt highlights that while it would be possible to apply morphing to various sizes of active HBMs and study whole-sequence rear-end simulations, more work on initial spinal curvature and model stabilisation would be needed first. As the active HBM requires a settling phase to reach a posture maintaining semi-equilibrium state before any braking or steering manoeuvre or crash intervention, it is hard to prescribe a certain backset or posture by just positioning the model, which complicates the reproducibility of such simulations.

Limitations

If the goal of being able to simulate whole-sequence rear-end impacts with active HBMs is achieved, it would allow for a holistic assessment of car seats and other parts of the restraint system. These systems interact with the occupant before, during and after the impact, and whole-sequence simulations could potentially lead to the design of novel systems and enhanced third-party assessment. However, to enable the current study, several assumptions had to be made and the limitations associated with them should be mentioned.

The muscle activation algorithm that was developed to model vehicle manoeuvre responses, had a number of underlying assumptions about the muscle spatial tuning, etc. [53]. In the present study, it was assumed that the muscle activations were changed during the braking phase, but that they remained constant during the impact. Using the APF muscle control algorithm during the impact phase was tested previously [17] and generates what seems to be too high muscle activations. For rear-end impacts as studied in the present manuscript, a human-like muscle activation scheme during impact is an important next step for more accurate HBM simulation.

In rear-end impacts, as it is of interest to study intervertebral motions, the initial posture of the model is important. It was observed that the spine of the HBM became more lordotic, Fig. C1 in Appendix C, during the initialisation phase, achieving a semi-stable posture by a combination of spine compression, ligament tension and muscle contraction. Future research would be needed to validate if this is a biofidelic posture-maintenance strategy, and even more so to generalise it to morphed HBMs.

In addition, no injury prediction was attempted for the present study. Instead, several measures that have been reported to correlate with the risk of whiplash injury, such as the initial backet, elongation of the spinal canal, the relative head–T1 motion and T1 accelerations were reported. A previous study with an active HBM [24] utilised the opposite approach and included as many criteria as possible, and while many of them could have been applied, here they were omitted as they remain unvalidated for the HBM used. A well established, tissue-level injury criteria that reflects some of the proposed injury mechanisms for whiplash injury would be most useful, but that remains to be developed for the present HBM. Intermediate steps that could be used for an FE HBM are possibly also measures as explored here with local intervertebral rotations, or additional local facet joint shearing motions that are possible to evaluate in simulations.

Moreover, only one occupant size, one crash pulse and crash direction and one seat were included in the study. The method used here could be expanded to answer questions regarding the influence of such variations, but it was decided that would fall outside of the scope of the present study.

V. CONCLUSION

This study demonstrated that utilising an active HBM in whole-sequence rear-end impact scenarios allowed for investigation of muscle activation effects and braking interventions for a car driver. Leveraging the ability of FE HBMs to be morphed to varying occupant sizes, in combination with modelling of active muscle response opens up the possibility for assessing the whole population of occupants and scenarios with varying sizes, shapes, and sitting postures, for both drivers and passengers. However, as discussed in the study, additional work is needed to ensure the initial posture of morphed models. As active HBMs with feedback control requires an initialisation and settling phase, achieving full control of the occupant's posture at the start of the crash phase is challenging. More work will be needed to ensure that such effects are occupant-specific and not just modelling artifacts.

Braking significantly affects occupant head-neck kinematics in the crash phase by increasing the backset, while interventions like the Electrical Reversible Retractor (ERR) can mitigate some of the backset increase. Muscle activations generated during the braking phase influenced local intervertebral segment rotations during the crash phase and the rebound kinematics.

VI. ACKNOWLEDGEMENTS

This work was carried out at SAFER, Vehicle and Traffic Safety Centre at Chalmers University of Technology, Gothenburg, Sweden, and funded by FFI-Strategic Vehicle Research and Innovation, by Vinnova, the Swedish Energy Agency, the Swedish Transport Administration and the Swedish vehicle industry.

VII. REFERENCES

[1] Stigson, H., Gustafsson, M., Sunnevång, C., Krafft, M., Kullgren, A. (2015) Differences in Long-Term Medical Consequences Depending on Impact Direction Involving Passenger Cars. *Traffic Injure Prevention*, **16**(sup1): pp. 133–139.

[2] Stigson, H., Boström, M., Kullgren, A. (2020) Health Status and Quality of Life among Road Users with Permanent Medical Impairment Several Years After the Crash. *Traffic Injury Prevention.* **21**(sup1): pp. S43–S48.

[3] Viano, D.C., Olsén, S. (2001) The Effectiveness of Active Head Restraint in Preventing Whiplash. *Journal of Trauma*, **51**(5): pp. 959–969.

[4] Jakobsson, L., Norin, H. (2004) AIS1 Neck Injury Reducing Effect of WHIPS (Whiplash Protection System). *Proceedings of the IRCOBI Conference*, Graz, Austria.

[5] Edwards, M.A., Brumbelow, M.L. (2023) Relationship of Whiplash Injury Metrics and Crash Pulse Severity to Injury Claim Rates. *Proc of the IRCOBI Conference*, Cambridge, England.

[6] Jakobsson, L., Lundell, B., Norin, H., Isaksson-Hellman, I. (2000) WHIPS-Volvo's Whiplash Protection Study. *Accident Analysis and Prevention*, **32**(2): pp. 307–319.

[7] Morris, A.P., Thomas, P. (1996) A Study of Soft Tissue Neck Injuries in the UK. *Proceedings of the ESV Conference*, Paper No. 96-S9-O-08, Melbourne, Australia.

[8] Jakobsson, L., Isaksson-Hellman, I., Lindman, M. (2008) WHIPS (Volvo Cars' Whiplash Protection System) – The Development and Real-World Performance. *Traffic Injury Prevention*, **9**(6): pp. 600–605.

[9] Jakobsson, L. (2004) Field Analysis of AIS1 Neck Injuries in Rear-end Car Impacts—Injury Reducing Effect of the WHIPS seat. *Journal of Whiplash Related Disorders*, **3**(2): pp. 37–54.

[10] Davidsson, J., Linder, A. *et al.* (1998) BioRID – A New Biofidelic Rear Impact Dummy, *Proceedings of the IRCOBI Conference*, Gothenburg, Sweden.

[11] Eriksson, L., Boström, O. (1999) Assessing the Influence of Crash Pulse, Seat Force Characteristics and Head Restraint Position on NICmax in Rear-End Crashes using a Mathematical BioRID dummy, *Proceedings of the IRCOBI Conference,* Sitges, Spain.

[12]Carlsson, A., Chang, F., *et al.* (2012) EvaRID - A 50th Percentile Female Rear Impact Finite Element Dummy Model. *Proceedings of the IRCOBI Conference,* Dublin, Ireland.

[13]Linder, A., Heinzl, P., *et al.* (2023) Open Source Tools for Road User Safety Assessment from the VIRTUAL Project. *Transportation Research Proceedings* **72**: pp. 423–430.

[14]Iraeus, J., Mishra, E., Östh, J. (2023) Comparison of Average Female and Male Active HBM Responses in Whole-Sequence Frontal Crash Simulations. *Proceedings of the IRCOBI Conference*, Cambridge, UK.

[15]Hwang, E., Hallman, J., *et al.* (2016) Rapid Development of Diverse Human Body Models for Crash Simulations through Mesh Morphing. *SAE Technical Paper* 2016-01-149.

[16]Jakobsson, L., Östh, J., Bohman, K. (2021) Rear-End Impact Assessment Expanded with Pre-Impact Posture Variations. *Proceedings of the IRCOBI Conference*, Online.

[17]Östh, J., Larsson, E., Jakobsson, J. (2022) Human Body Model Muscle Activation Influence on Crash Response. *Proceedings of the IRCOBI Conference*, Porto, Portugal.

[18]Iwamoto, M., Nakahira, Y., Kimpara, H., Sugiyama, T. (2012) Development of a Human Body Finite Element Model with Multiple Muscles and their Controller for Estimating Occupant Motions and Impact Responses in Frontal Crash Situations. *Stapp Car Crash Journal,* **56**: pp. 231–268.

[19]Kato, D., Nakahira, Y., Atsumi, N., Iwamoto, M. (2018) Development of Human-Body Model THUMS Version 6 containing Muscle Controllers and Application to Injury Analysis in Frontal Collision after Brake Deceleration*. Proceedings of the IRCOBI Conferenc*e, Athens, Greece.

[20]Matsuda, T., Yamada, K., Hayashi, S., Kitagawa, Y. (2018) Simulation of Occupant Posture Changes due to Evasive Manoeuvres and Injury Predictions in Vehicle Frontal and Side Collisions. *Proceedings of the IRCOBI Conference*, Athens, Greece.

[21]Meijer, R., Rodarius, C., Adamec, J., van Nunen, E., van Rooij, L. (2008) A First step in Computer Modelling of the Active Human Response in a Far-Side Impact. *International Journal of Crashworthiness,* **13**(6): pp. 643–652.

[22]Wass, J., Östh, J., Jakobsson, L. (2022) Active Human Body Model Simulations of Whole-Sequence Braking and Far-Side Impact Configurations. *Proceedings of the IRCOBI Conference*, Porto, Portugal.

[23]Gonzalez-Garcia, M., Weber, J., Peldschus, S. (2021) Potential Effect of Pre-Activated Muscles under a Far-Side Lateral Impact. *Traffic Injury Prevention,* **22**: pp. S148–152.

[24]Broos, J., Meijer, R. (2016) Simulation Method for Whiplash Injury Prediction using an Active Human Model. *Proceedings of the IRCOBI Conference*, Malaga, Spain.

[25]Östh, J., Brolin, K., Bråse, D. (2015) A Human Body Model with Active Muscles for Simulation of Pretensioned Restraints in Autonomous Braking Interventions. *Traffic Injury Prevention,* **16**(3): pp. 304–313.

[26]Chancey, V. C., Nightingale, R. W., van Ee, C., Knaub, K. E., Myers, B. S. (2003) Improved Estimation of Human Neck Tensile Tolerance: Reducing the Range of Reported Tolerance Using Anthropometrically Correct Muscles and Optimized Physiologic Initial Conditions. *Stapp Car Crash Journal,* **47**: pp. 135–153.

[27]Behr, M., Arnoux, P.-J., Serre, T., Thollon, L., Brunet, C. (2006) Tonic Finite Element Model of the Lower Limb. *J Biomechical Engineering,* **128**: pp. 223–228.

[28]Sugiyama, T., Kimpara, H., *et al.* (2007) Effects of Muscle Tense on Impact Responses of Lower Extremity. *Proceedings of the IRCOBI Conference*, Maastricht, the Netherlands.

[29]Meijer, R., van Hassel, E., *et al.* (2012) Development of a Multi-Body Human Model that Predicts Active and Passive Human Behaviour. *Proceedings of the IRCOBI Conference*, Dublin, Ireland.

[30]Devane, K., Johnson, D., Gayzik, F.S. (2019) Validation of a Simplified Human Body Model in Relaxed and Braced Conditions in Low-Speed Frontal Sled Tests. *Traffic Injury Prevention,* **20**(8): pp. 832–837.

[31]Fice, J.B., Cronin, D.S., Panzer, M.B. (2011) Cervical Spine Model to Predict Capsular Ligament Response in Rear Impact. *Annals of Biomedical Engeering* **39**(8): pp. 2152–2162.

[32]Ejima, S., Ono, K., Kaneoka, K., Fukushima, M. (2005) Development and Validation of the Human Neck Muscle Model under Impact Loading. *Proceedings of the IRCOBI Conference*, Prague, Czech Republic.

[33]Brault, J.R., Siegmund, G.P., Wheeler, J.B. (2000) Cervical Muscle Response during Whiplash: Evidence of a Lengthening Muscle Contraction. *Clinical Biomechanics* **15**: pp. 426–435.

[34]Iraeus, J., Brynskog, E., *et al.* (2024) *Development of SAFER HBM v11.* Chalmers University of Technology, Gothenburg, Sweden. Report 2024:06. https://doi.org/10.5281/zenodo.10886711

[35]Jakobsson, L., Lindman, M., Björklund, M., Victor, T. (2015) Rear-End Impact – Crash Prevention and Occupant Protection, *Proceedings of the IRCOBI Conference*, Lyon, France.

[36]Schneider, L. W., Robbins, D. H., Pflüg, M. A., Snyder, R. G. (1983) *Development of anthropometrically based design specifications for an advanced adult anthropomorphic dummy family, Final Report*. University of Michigan Transportation Research Institute, Ann Arbor, MI, USA.

[37]Iraeus, J., Pipkorn, B. (2019) Development and Validation of a Generic Finite Element Ribcage for Strain Based Fracture Prediction. *Proceedings of the IRCOBI Conference,* Florence, Italy.

[38]Kleiven, S. (2007) Predictors for Traumatic Brain Injuries Evaluated through Accident Reconstructions. *Stapp Car Crash Journal,* **51**.

[39]Brynskog, E., Iraeus, J., Pipkorn, B., Davidsson, J. (2022) Population Variance in Pelvic Response to Lateral Impacts – A Global Sensitivity Analysis. *Proceedings of the IRCOBI Conference*, Porto, Portugal.

[40]Iraeus, J., Niranjan Poojary, Y., Jaber, l., John, J., Davidsson, J. (2023) A New Open-Source Finite Element Lumbar Spine Model, Its Tuning and Validation, and Development of a Tissue-based Injury Risk Function for Compression Fractures. *Proceedings of the IRCOBI Conference*, Cambridge, UK.

[41]Larsson, E., Iraeus, J., *et al.* (2019) Active Human Body Model Predictions Compared to Volunteer Response in Experiments with Braking, Lane Change, and Combined Manoeuvres. *Proceedings of the IRCOBI Conference*, Florence, Italy.

[42]Bärgman, J., Svärd, M., Lundell., S., Hartelius, E. (2024) Methodological Challenges of Scenario Validation: A Rear-end Crash Causation Model for Virtual Safety Assessment. *Transportation Research Part F: Traffic Psychology and Behaviour* **104**: pp. 374–410.

[43]IIHS (2020) *Vehicle Seat/Head Restraint Evaluation Protocol, Dynamic Criteria (Version VI)*. Insurance Institute for Highway Safety, Ruckersville, VA, USA.

[44]Olsson, I., Bunketorp, O. *et al.* (1990) An In-Depth Study of Neck Injuries in Rear-end Collisions. *Proceedings of the IRCOBI Conference*, Bron, France, pp. 269–280.

[45]Boström, O., Svensson, M. *et al.* (1996) A New Neck Injury Criterion Candidate – Based on Injury Findings in the Cervical Spinal Ganglia after Experimental Neck Extension Trauma. *Proceedings of the IRCOBI Conference,* Dublin, Ireland.

[46]Ono, K. and Kaneoka, K. (1997) Motion Analysis of Human Cervical Vertebrae during Low Speed Rear Impacts by the Simulated Sled. *Proceedings of the IRCOBI Conference*, Hannover, Germany.

[47]Stemper, B.D., Yoganandan, N., Pintar, F.A. (2003) Gender Dependent Cervical Spine Segmental Kinematics during Whiplash. *Journal of Biomechanics* **36**: pp. 1281–1289.

[48]Von Koch, M., Kullgren, A., Lie., A., Nygren, Å., Tingvall, C. (1995) Soft Tissue Injury of the Cervical Spine in Rear-End and Frontal Car Collisions. *Proc IRCOBI Conference*, Brunnen, Switzerland.

[49]Östh K.J.H., Olafsdóttir, J.M., Davidsson, J., Brolin, K. (2013) Driver Kinematic and Muscle Responses in Braking Events with Standard and Reversible Pre-tensioned Restraints: Validation Data for Human Models. *Stapp Car Crash Journal,* **57**: pp. 1–41.

[50]Magnusson, M.L., Pope, M.H. *et al.* (1999) Cervical Electromyographic Activity during Low-Speed Rear Impact. *European Spine Journal* **8**: pp. 118–125.

[51]Dehner, C., Schick, S., Kraus, M., Hell, W., Kramer, M. (2013) Muscle Activity Influence on the Kinematics of the Cervical Spine in Rear-End Sled Tests in Female Volunteers. *Traffic Injury Prevention* **14**(4): pp. S369–377.

[52]Ólafsdóttir, J.M., Brolin, K., Blouin, J.-S., Siegmund, G.P. (2015) Dynamic Spatial Tuning of Cervical Muscle Reflexes to Multidirectional Seated Perturbations. *Spine* **40**(4): pp. E211–E219.

[53]Ólafsdóttir, J. M., Östh, J., Brolin, K. (2019) Modelling Reflex Recruitment of Neck Muscles in a Finite Element Human Body Model for Simulating Omnidirectional Head Kinematics. *Proceedings of the IRCOBI Conference*, Florence, Italy.

[54]Hartlen, D.C., Cronin, D.S. (2022) Arc-Length Re-Parameterization and Signal Registration to Determine a Characteristic Average and Statistical Response Corridors of Biomechanical Data. *Frontiers in Bioengeering and Biotechnology* **10**: 843148.

[55]OpenVT (2024) HBM4VT Validation Catalogue. Online: https://openvt.eu/EuroNCAP/hbm4vt-validation-catalogue. Accessed 2025-05-28.

VIII. APPENDIX A – HBM PRE-CRASH VALIDATION

The updated SAFER HBM v11 M50 was validated for driver autonomous brake intervention kinematics using a simulation setup developed by [41], complemented with a steering wheel for the present study. First a 650 ms initialisation phase was simulated, during which the model was settled under gravity with its arms and feet positioned using cable elements. Then a 2500 ms 1.1 g braking events with vehicle accelerations and restraint parameters (Standard Belt (SB) and 170 N reversible Pre-Tension (PT)) from the volunteer tests [49] was simulated.

Fig A1. Driver autonomous brake intervention validation setup [41] with the SAFER HBM v11 M50.

The HBM response was compared with test data from 11 males (average stature 178 cm, average weight 77 kg). The boundary conditions and occupant kinematics responses from both simulation and test are shown in Fig A2–Fig. A6. Objective comparison metrics were calculated in the form of ISO/TS 18571 Score in comparison with the pointwise volunteer average and Ellipse Score using arc-length average corridors [54]. Both ISO Scores and Ellipse Score was calculated using python scripts from the Euro NCAP HBM Certification Catalogue [55].

In general, the seat-belt forces were high, on border of the upper ± 1 Standard Deviation (SD) corridor, indicating a weaker HBM response that relied more on the seat-belt for restraint than most of the volunteers. The same pattern was seen for the X displacement which was on the upper border, meaning that the HBMs response was comparable to the more compliant volunteers. The ISO Score calculation does not use the volunteer data corridor but rather an inner and outer corridor based on the peak value for the average volunteer signal, which is why the HBM ISO Scores, Table AI, were low, with averages of 0.4 for all simulations. The arc-length average corridors, Fig. A6, were similar to the pointwise corridors and as the Ellipse Scores also accounts for the corridors these were higher than the ISO Scores, on average 0.46 and 0.63 for the SB and PT load case, respectively.

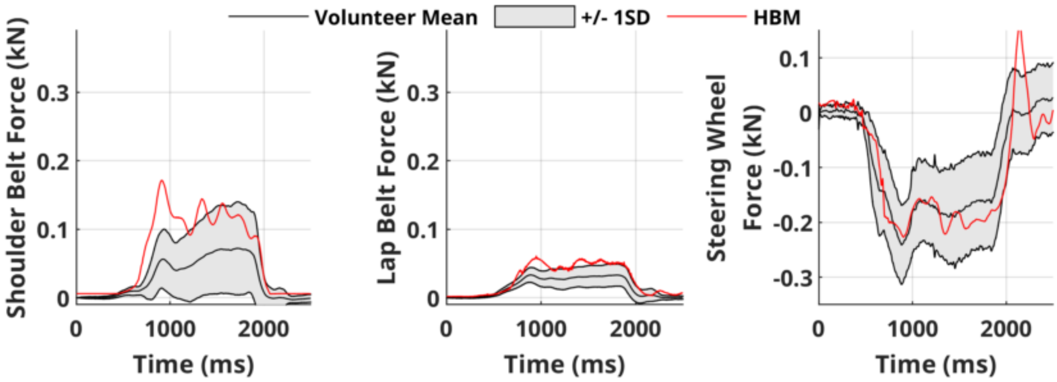

Fig A2. SAFER HBM v11 M50 boundary condition forces for the autobrake with Standard Belt (SB) validation load case.

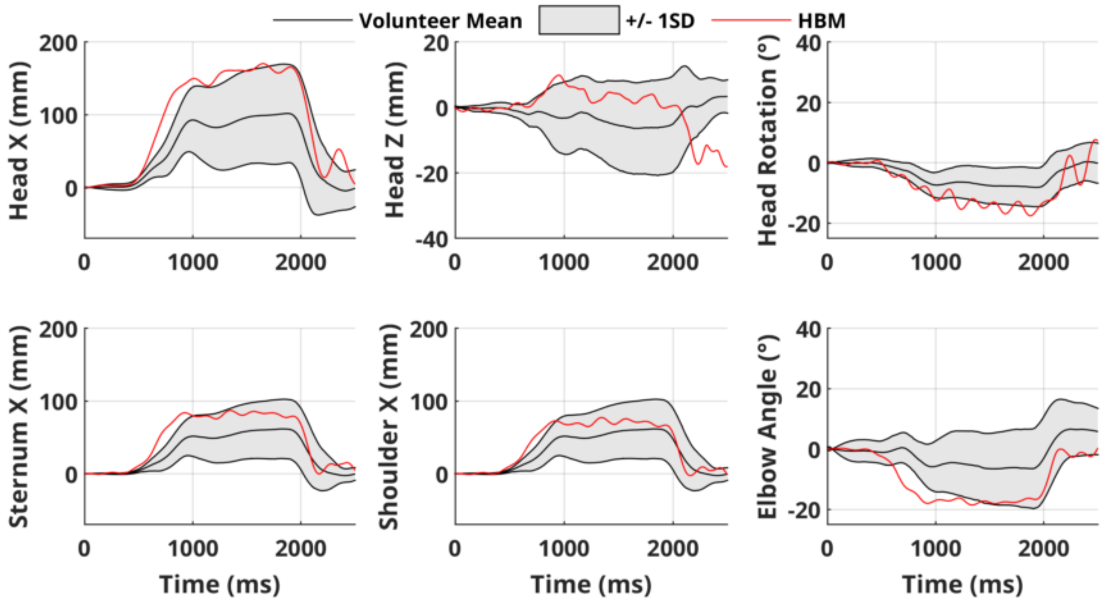

Fig A3. SAFER HBM v11 M50 kinematics for the autobrake with Standard Belt (SB) validation load case.

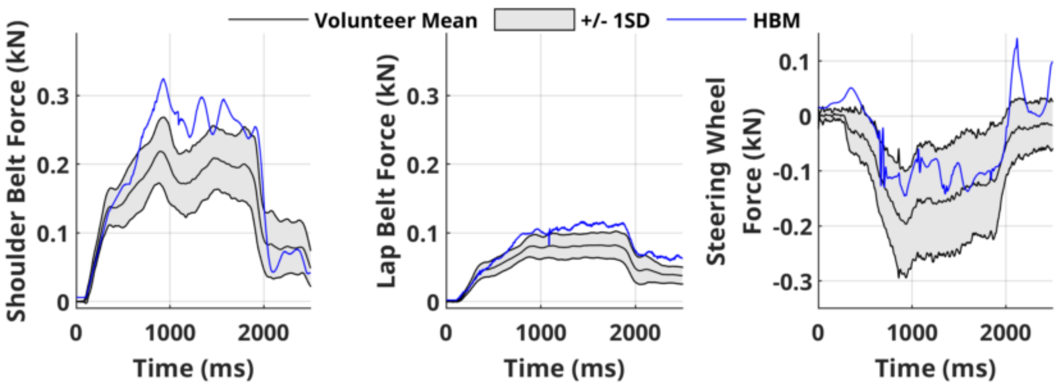

Fig A4. SAFER HBM v11 M50 boundary condition forces for the autobrake with Pre-Tensioned (PT) validation load case.

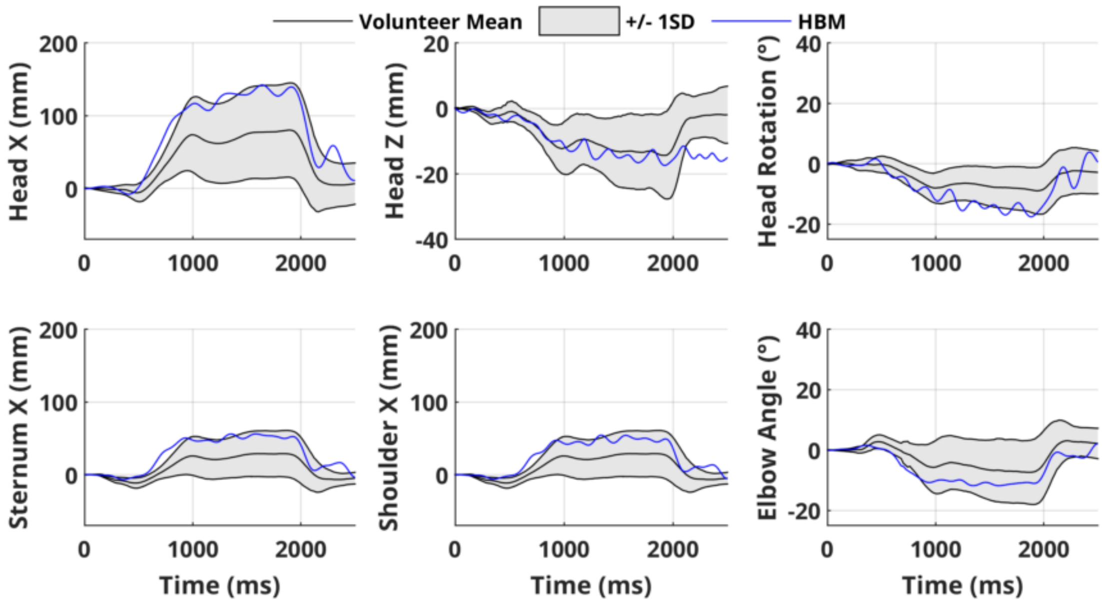

Fig A5. SAFER HBM v11 M50 kinematics for the autobrake with Pre-Tensioned (PT) validation load case.

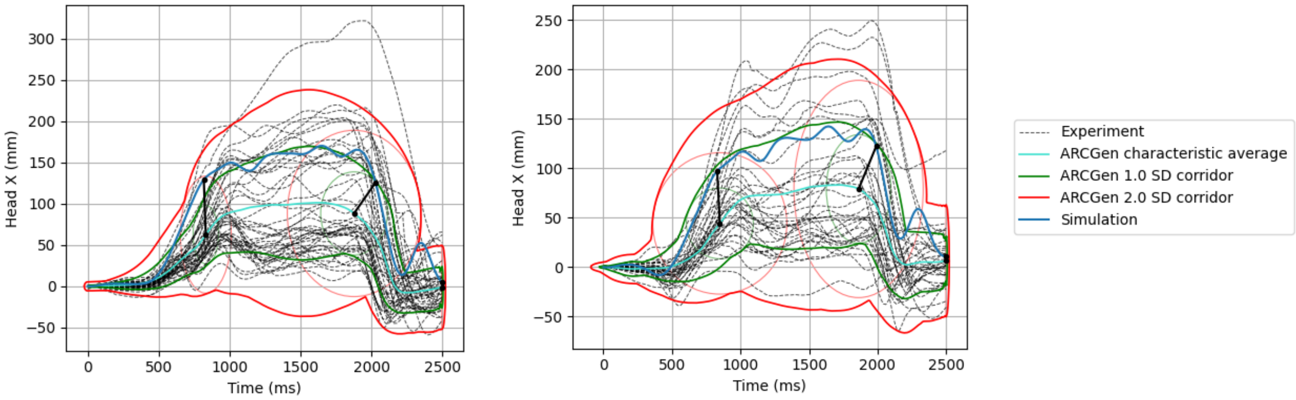

Fig A6. Example of arc-length [54] corridors for the head X displacement for the autobrake with Standard Belt (SB) load case (left) and with Pre-tensioned Belt (PT) load case (right).

TABLE AI
OBJECTIVE RATING METRICS FOR ACTIVE SAFER HBM V11 RESPONSES COMPARED WITH THE VOLUNTEER AVERAGE RESPONSE.
SB = STANDARD BELT. PT = PRE-TENSIONED BELT. ISO = ISO/TS 18571 SCORE. ES = ELLIPSE SCORE.

Load Case	**Score Type**	**Shoulder Belt Force**	**Lap Belt Force**	**Steering Wheel Force**	**Head X**	**Head Z**	**Head Rotation**	**Sternum X**	**Shoulder X**	**Elbow Angle**	**Average**
SB	ISO	0.35	0.39	0.67	0.40	0.08	0.29	0.48	0.61	0.31	0.40
	ES	0.09	0.1	0.34	0.36	0.72	0.38	0.65	0.61	0.85	0.46
	ES DTW	0.79	0.56	0.80	0.89	0.85	0.90	0.88	0.92	0.98	0.84
PT	ISO	0.56	0.46	0.49	0.36	0.40	0.34	0.32	0.30	0.37	0.40
	ES	0.32	0.08	0.60	0.71	0.85	0.66	0.71	0.77	0.95	0.63
	ES DTW	0.83	0.59	0.90	0.98	0.94	0.98	0.94	0.96	1.0	0.90

IX. APPENDIX B – HBM MUSCLE ACTIVATIONS

The muscle activations for the SAFER HBM were calculated for eight spatial tuning groups for the cervical controller [51], Fig. B1, and for four groups for the lumbar controller [41], Fig. B2. All the muscles in each group, on the same side of the sagittal midplane of the body had the same activation level, and the resulting muscle activations in the simulation were presented and analysed in these groups.

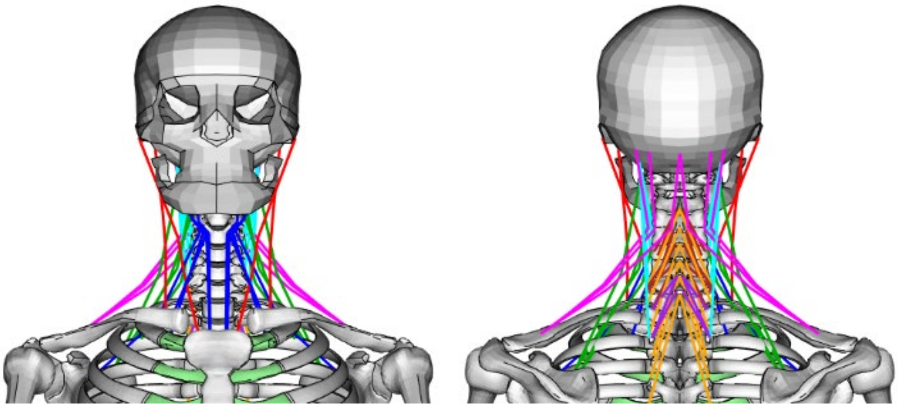

Fig. B1. Cervical muscle spatial tuning groups [51]. Red: Sternocleidomastoideus (SCM) group. Blue: Sternohyoid (STH) group. Green: Levator Scapulae (LS) group. Magenta: Trapezius (TRAP) group. Cyan: Semispinalis Capitis (SCap) group. Orange: Semispinalis Cervicis (SCerv) group. Brown: C4 level Multifidus (CM-C4) group. Purple: C6 level Multifidus (CM-C6) group.

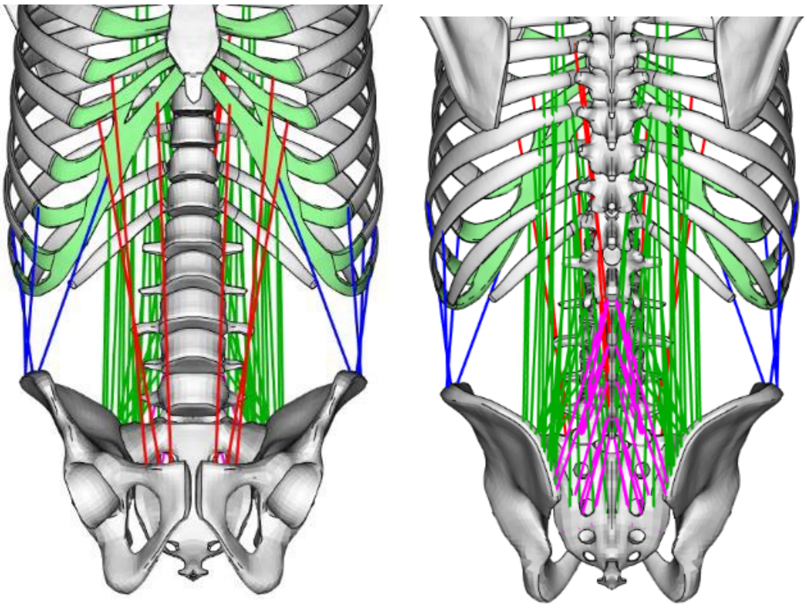

Fig. B2. Lumbar muscle spatial tuning groups [41]. Red: Rectus Abdominis (RA) group. Blue: Obliques (OBL) group. Green: Lumbar Erector Spinae (LES) group. Magenta: Lumbar Multifidus group (LMF).

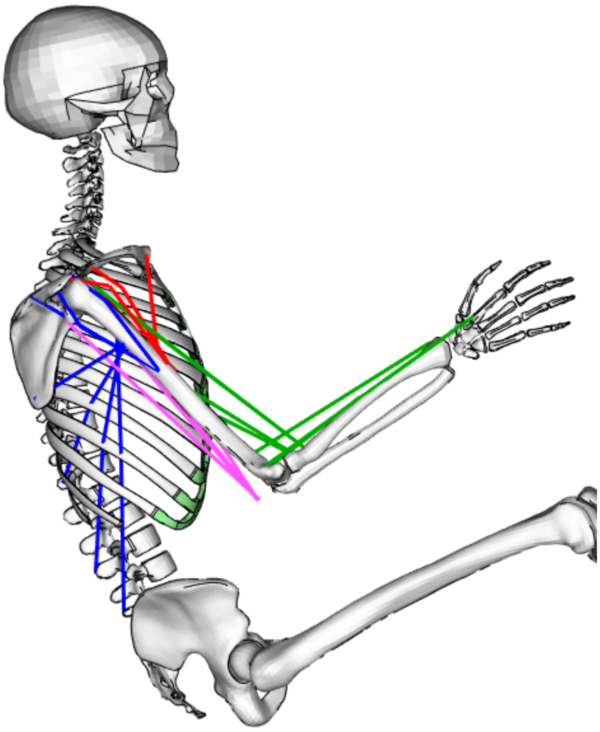

Fig. B3. Upper extremity muscle spatial tuning groups [25]. Red: Shoulder Flexor (Flex) group. Blue: Shoulder Extensor (Ext) group. Green: Elbow Flexor (Flex) group. Magenta: Elbow Extensor (Ext) group.

TABLE BI
Muscle activations in % at the end of the braking or initialisation phase, kept constant during the rear-end impact phase. Muscle name abbreviations according to Figs B1–B3.

	Cervical Flexors				Cervical Extensors												Shoulder				Elbow				Trunk Flexors				Trunk Extensors			
Sim.	SCM		STH		LS		TRAP		SCap		SCerv		CMC4		CMC6		Flex		Ext		Flex		Ext		RA		OBL		LES		LMF	
	L	R	L	R	L	R	L	R	L	R	L	R	L	R	L	R	L	R	L	R	L	R	L	R	L	R	L	R	L	R	L	R
1	11	11	12	12	1	1	1	1	5	5	3	3	1	1	2	2	4	4	3	3	2	2	7	8	17	17	2	2	5	5	5	5
2	6	8	4	4	8	9	7	10	100	100	68	72	30	29	50	55	10	13	3	3	2	2	32	39	5	5	6	6	7	14	7	14
3	4	4	4	4	4	4	3	4	51	54	31	31	13	13	23	23	4	10	3	3	2	5	11	50	5	8	7	4	14	5	14	5
4	0	0	0	0	0	0	0	0	0	0	0	0	0	0	0	0	0	0	0	0	0	0	0	0	0	0	0	0	0	0	0	0
5	0	0	0	0	0	0	0	0	0	0	0	0	0	0	0	0	0	0	0	0	0	0	0	0	0	0	0	0	0	0	0	0

X. APPENDIX C – IMAGE TIME SERIES

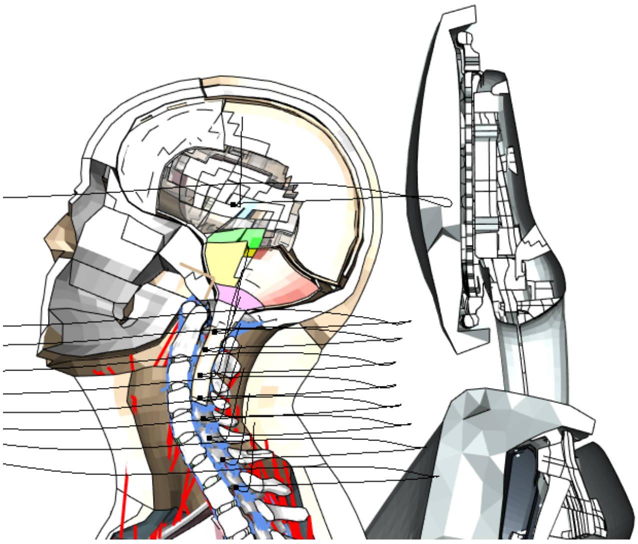

Fig. C1. The HBM at start of the rear-end impact for Sim. 1 and Sim. 4. The thin lines show the head CoG and spinal canal marker trajectories for Sim. 1.

S	T=0 ms	T=150 ms	T=300 ms	T=450 ms	T=600 ms
2	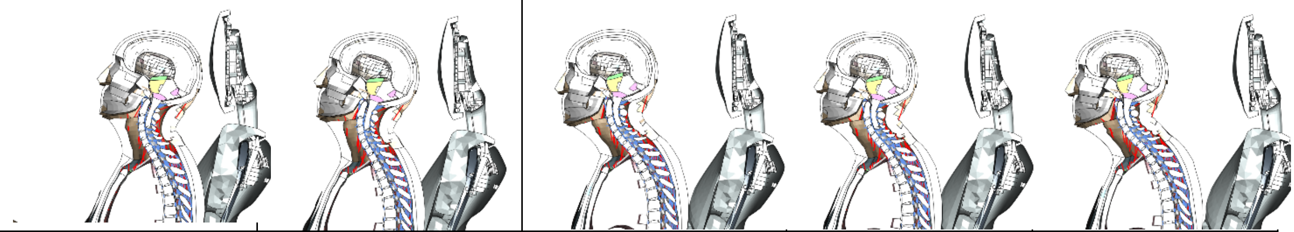				
3	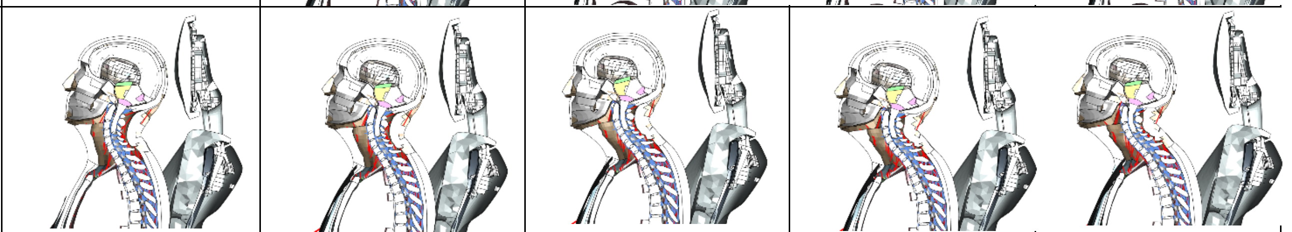				

Fig. C2. Time series of the braking for Simulations (S) 2 and 3, starting from after the initialisation phase, Fig. 2.

S	T=0 ms	T=50 ms	T=100 ms	T=150 ms	T=200 ms	T=300 ms	T=400 ms
1	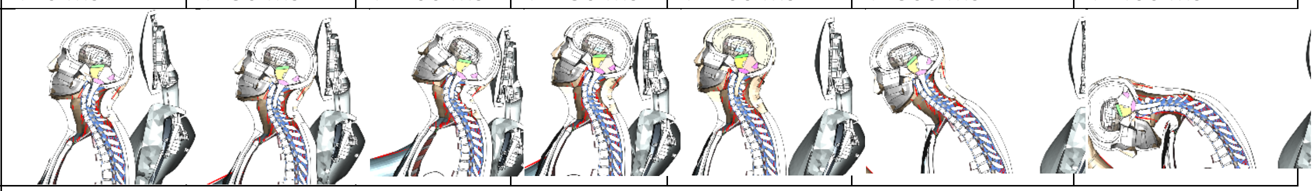						
2	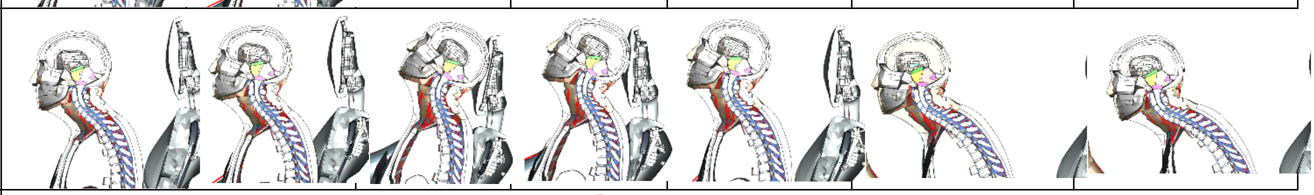						
3	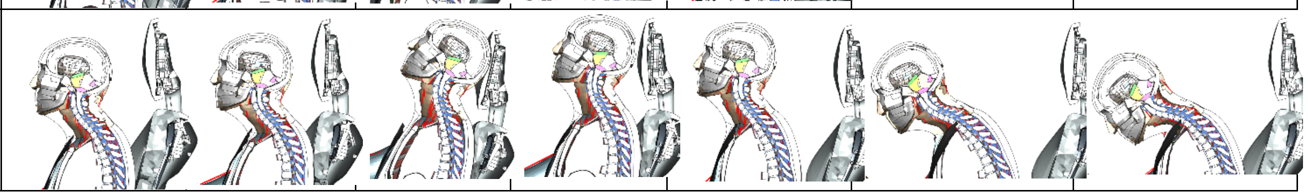						

4	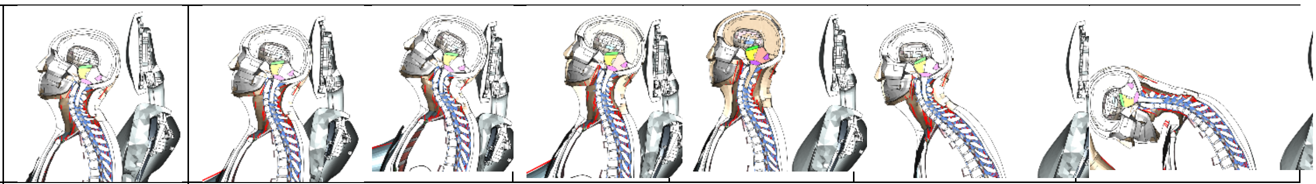
5	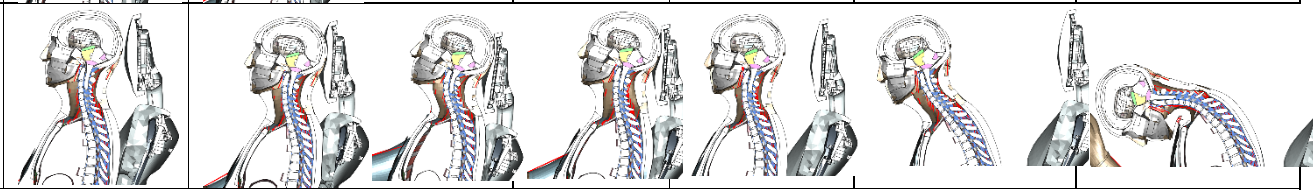

Fig. C3. Time series of the rear-end impact for Simulations (S) 1–5, in impact time, Fig. 2.

XI. APPENDIX D – PASSENGER OCCUPANT SIMULATIONS

To illustrate the difference between a driver and a passenger occupant, Sim. 1 to Sim. 3 (Table I) was repeated with the hands positioned in the lap instead of on the steering wheel, Fig. D1, and excluding arm muscle activation.

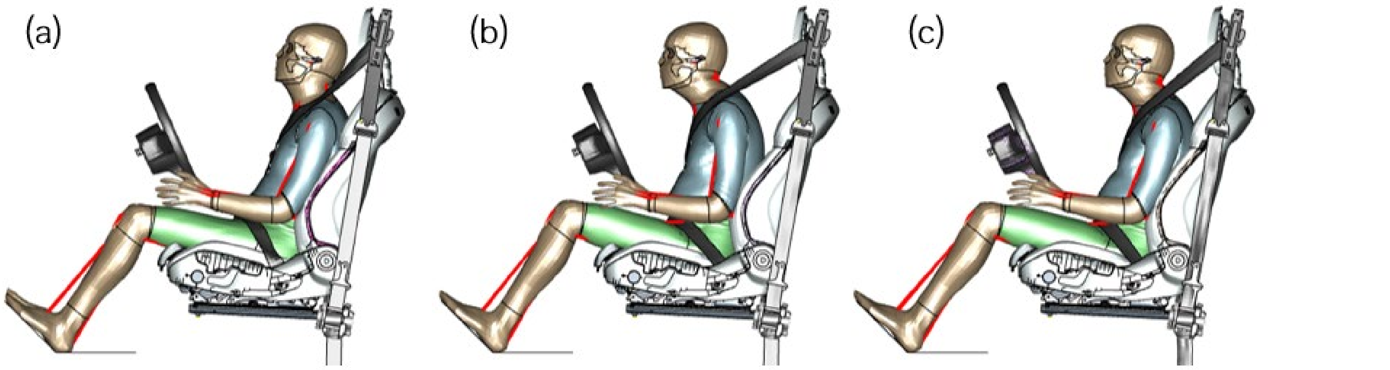

Fig. D1. HBM posture at start of impact for the repeated Sim. 1 (a), Sim. 2 (b) and Sim. 3 (c) with arms in the lap instead of on the steering wheel and without arm muscle activation.

The removal of the hand constraint to the steering wheel led to a more forward initial position for all simulations, Table DI, which also led to later head contact and higher peak accelerations and relative Head–T1 velocity compared with the driver occupant (Table II).

TABLE DI
SUMMARY OF INITIAL GEOMETRY AND PEAK KINEMATIC RESPONSES. ACC. = ACCELERATION. VEL. = VELOCITY. PASS. = PASSENGER OCCUPANT WITH HANDS IN THE LAP INSTEAD OF ON THE STEERING WHEEL

	Backset (mm)			Head-Head Restraint Interaction during Impact Time		Min Head–T1 X acc. (g)	Max Head–T1 X acc. (g)	Min Head–T1 X vel. (m/s)	Spinal Canal Length (mm)		Peak Intervertebral Flexion (+)		Peak Intervertebral Extension (-)	
Sim.	Initial	After Settling	At Start of Impact	Contact (ms)	Rebound (ms)				At Start of Impact	Peak	Level	(°)	Level	(°)
1 - Pass	12	46	46	55	148	-6.5	6.4	-1.0	109	129	C6C7	4.9	C2C3	-2.0
2 - Pass	12	46	220	98	163	-14.2	20.3	-3.0	109	114	C3C4	4.3	C6C7	-3.9
3 - Pass	12	46	119	75	145	-11.9	16.0	-2.5	112	128	C3C4	2.5	C7T1	-3.0

Figures D2–13 show a comparison between the driver and passenger occupant simulations for the spinal kinematics, the head–T1 kinematics, the spinal canal length and the cervical spine segment rotations.

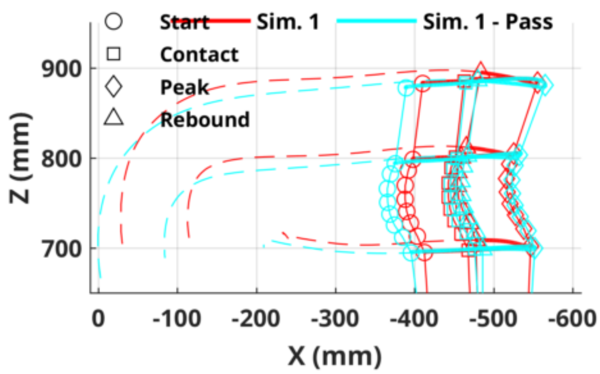

Fig. D2. The HBM spinal kinematics in Sim. 1 and the repeated Sim. 1 as a passenger during the rear-end impact. The upper most marker is the head CoG, the lower most in the centre of the spinal canal of T1. The thick solid trajectories show the loading phase, and the thin dashed show the rebound trajectories.

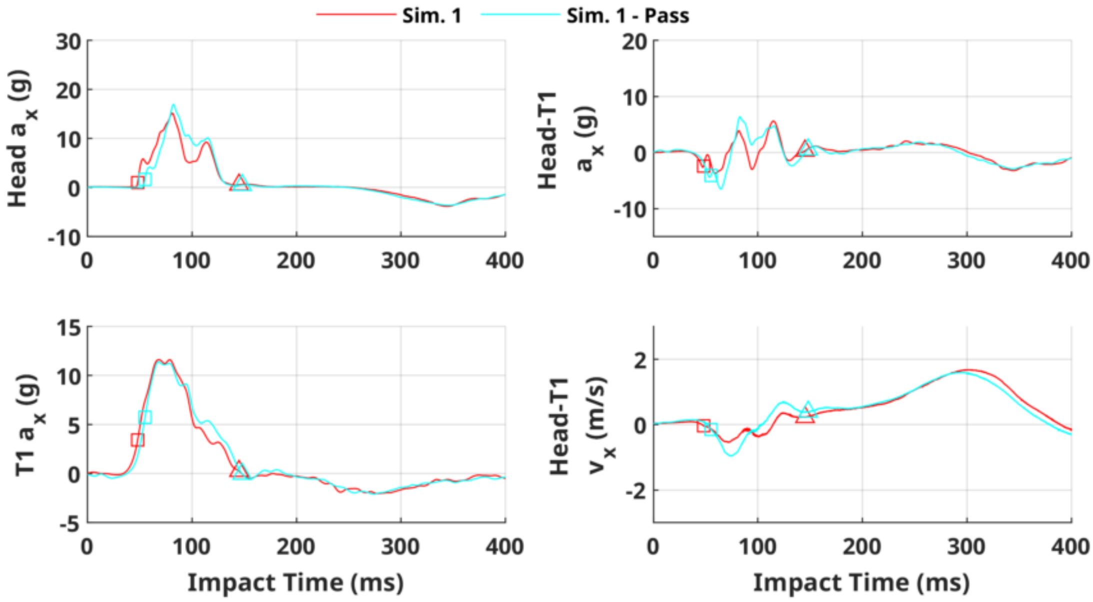

Fig. D3. The HBM head–T1 rear-end impact kinematics in Sim. 1 and the repeated Sim. 1 as a passenger. The square marker indicates the head-to-head restraint contact time, and the triangle timing of rebound when the head left the head-restraint.

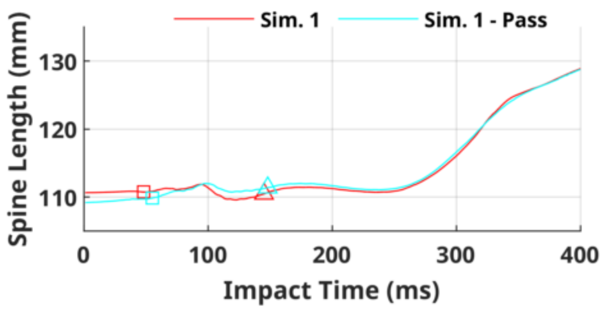

Fig. D4. The HBM cervical spine length during the rear-end impact for Sim. 1 and the repeated Sim. 1 as a passenger, calculated as the Euclidean distance between the C1–T1 vertebra markers (see also Fig. 3). The square marker indicates the head-to-head restraint contact time, and the triangle timing of rebound when the head left the head-restraint.

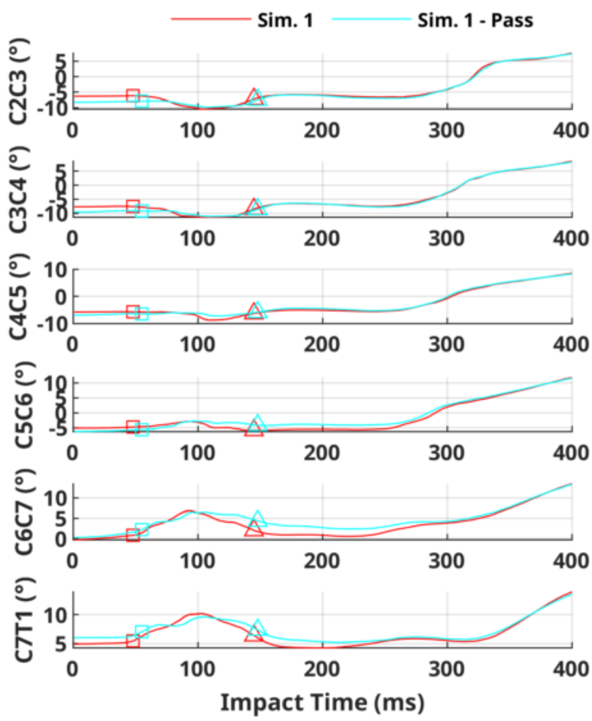

Fig. D5. The HBM cervical spine segment rotations during the rear-end impact in Sim. 1 and the repeated Sim. 1 as a passenger. The square marker indicates the head-to-head restraint contact time, and the triangle timing of rebound when the head left the head-restraint.

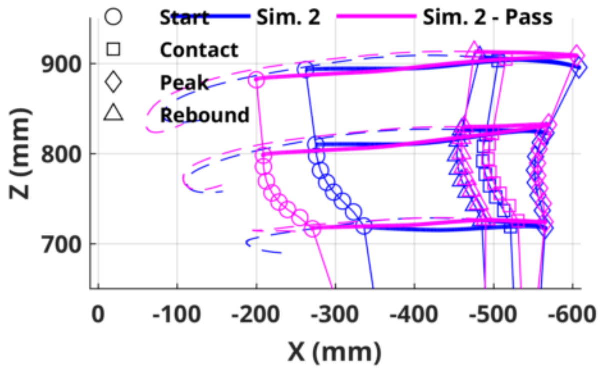

Fig. D6. The HBM spinal kinematics in Sim. 2 and the repeated Sim. 2 as a passenger during the rear-end impact. The upper most marker is the head CoG, the lower most in the centre of the spinal canal of T1. The thick solid trajectories show the loading phase, and the thin dashed show the rebound trajectories.

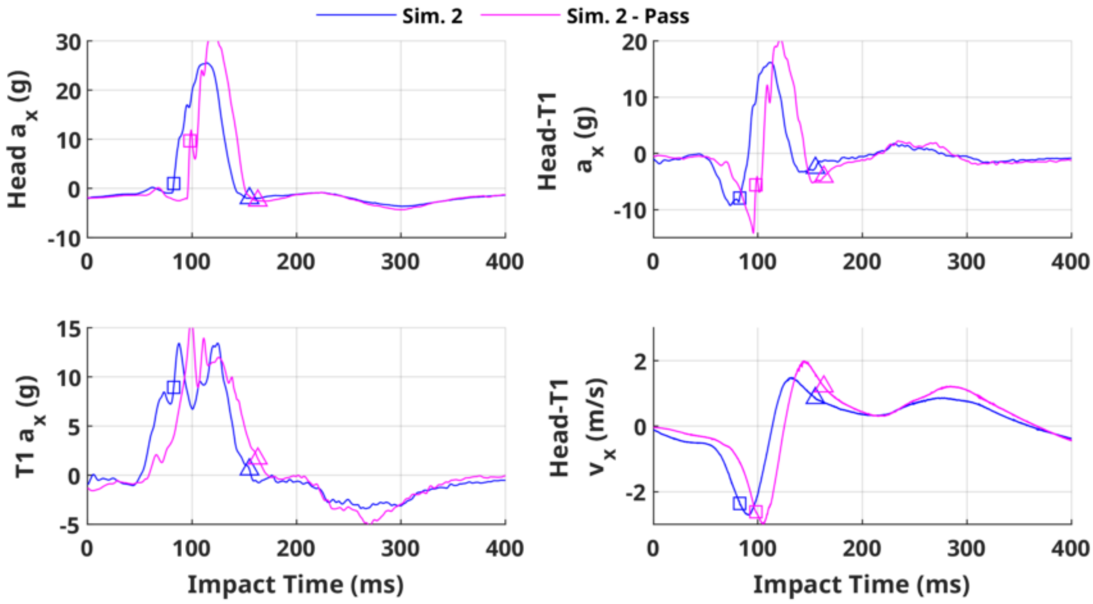

Fig. D7. The HBM head–T1 rear-end impact kinematics in Sim. 2 and the repeated Sim. 2 as a passenger. The square marker indicates the head-to-head restraint contact time, and the triangle timing of rebound when the head left the head-restraint.

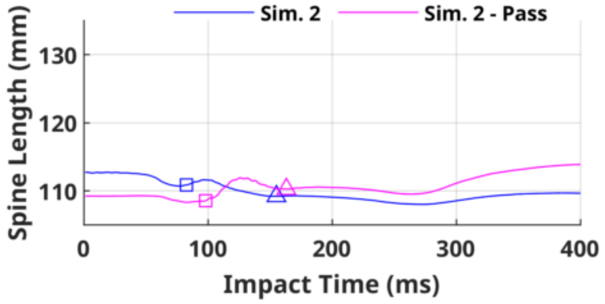

Fig. D8. The HBM cervical spine length during the rear-end impact for Sim. 2 and the repeated Sim. 2 as a passenger, calculated as the Euclidean distance between the C1–T1 vertebra markers (see also Fig. 3). The square marker indicates the head-to-head restraint contact time, and the triangle timing of rebound when the head left the head-restraint.

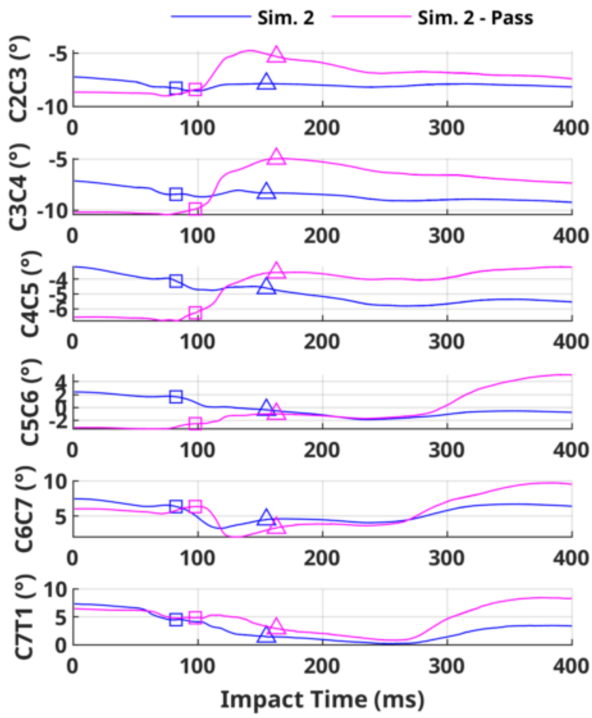

Fig. D9. The HBM cervical spine segment rotations during the rear-end impact in Sim. 2 and the repeated Sim. 2 as a passenger. The square marker indicates the head-to-head restraint contact time, and the triangle timing of rebound when the head left the head-restraint.

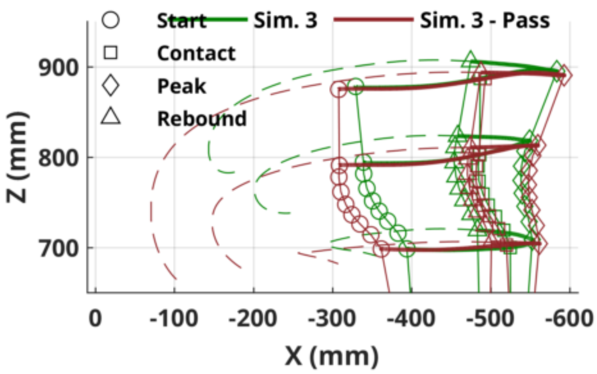

Fig. D10. The HBM spinal kinematics in Sim. 3 and the repeated Sim. 3 as a passenger during the rear-end impact. The upper most marker is the head CoG, the lower most in the centre of the spinal canal of T1. The thick solid trajectories show the loading phase, and the thin dashed show the rebound trajectories.

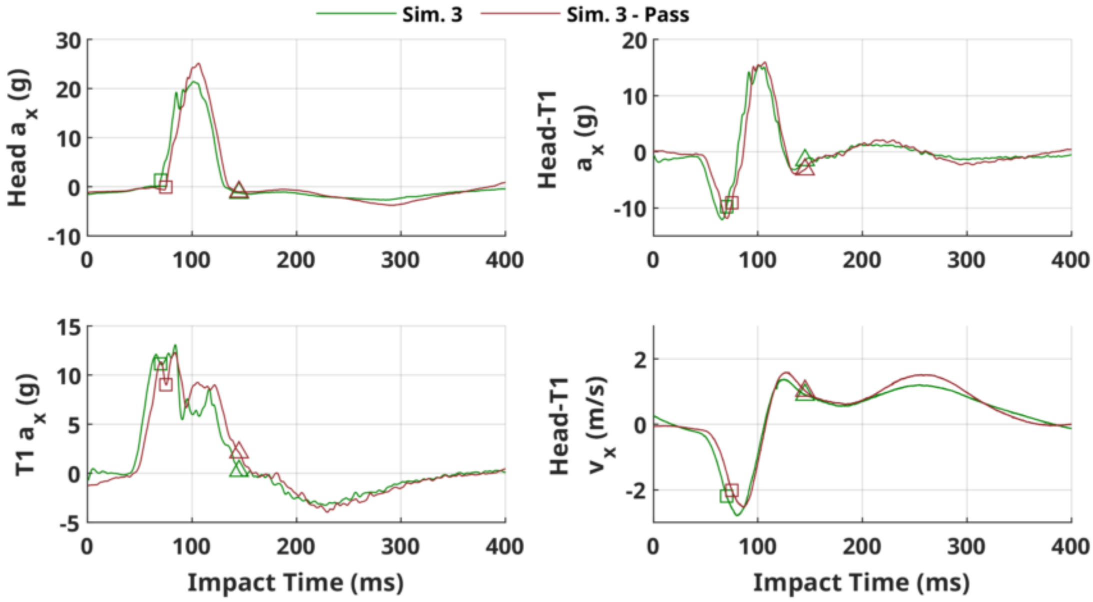

Fig. D11. The HBM head–T1 rear-end impact kinematics in Sim. 3 and the repeated Sim. 3 as a passenger. The square marker indicates the head-to-head restraint contact time, and the triangle timing of rebound when the head left the head-restraint.

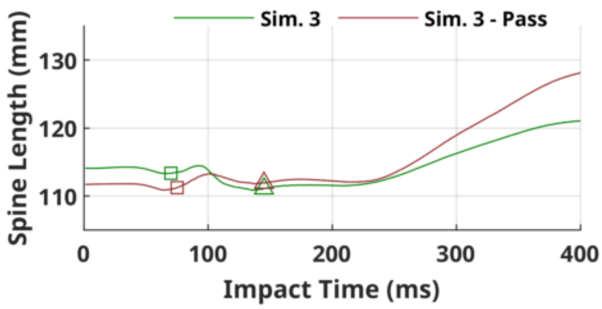

Fig. D12. The HBM cervical spine length during the rear-end impact for Sim. 3 and the repeated Sim. 3 as a passenger, calculated as the Euclidean distance between the C1–T1 vertebra markers (see also Fig. 3). The square marker indicates the head-to-head restraint contact time, and the triangle timing of rebound when the head left the head-restraint.

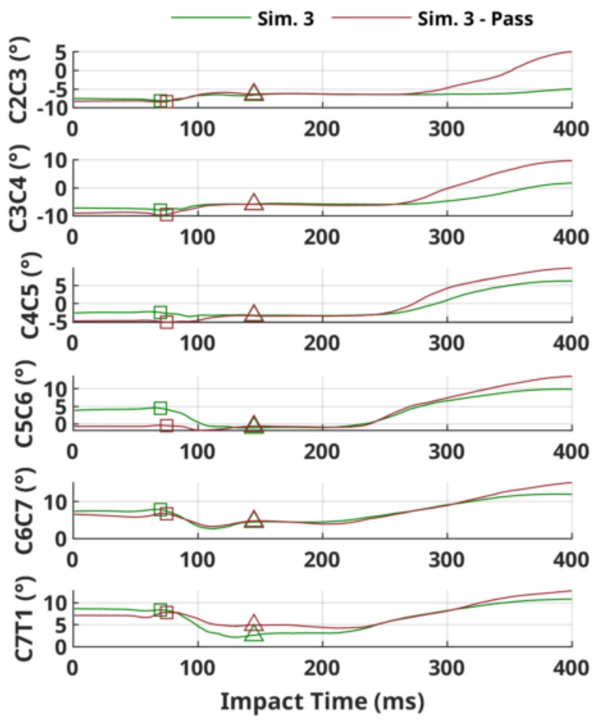

Fig. D13. The HBM cervical spine segment rotations during the rear-end impact in Sim. 3 and the repeated Sim. 3 as a passenger. The square marker indicates the head-to-head restraint contact time, and the triangle timing of rebound when the head left the head-restraint.

XII. APPENDIX E – SWITCH OFF OF MUSCLES AFTER BRAKING

To illustrate the effect of muscle activation also in the whole-sequence simulations including the braking, Sim. 2 was repeated with the muscle activations being switched off at the start of the impact time. This led to a larger difference in cervical spine response than for Sim. 4 which included the same switch off but without the braking manoeuvre. When starting in the forward position and with the muscle activations turned off, the spine lengthened and straightened substantially, Fig. E1 and Fig. E3–4. The Head–T1 kinematics, Fig. E2, where not affected as much.

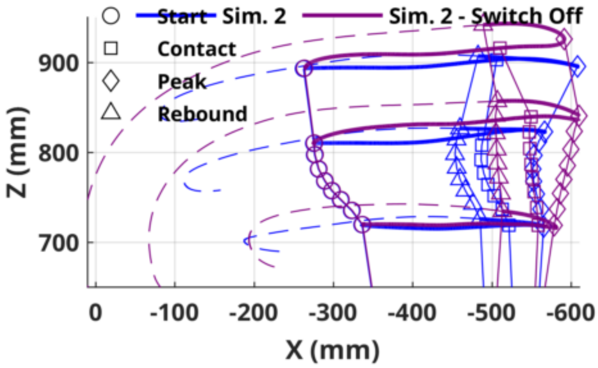

Fig. E1. The HBM spinal kinematics in Sim. 2 and the repeated Sim. 2 with muscle activations turned off at the start of impact. The upper most marker is the head CoG, the lower most in the centre of the spinal canal of T1. The thick solid trajectories show the loading phase, and the thin dashed show the rebound trajectories.

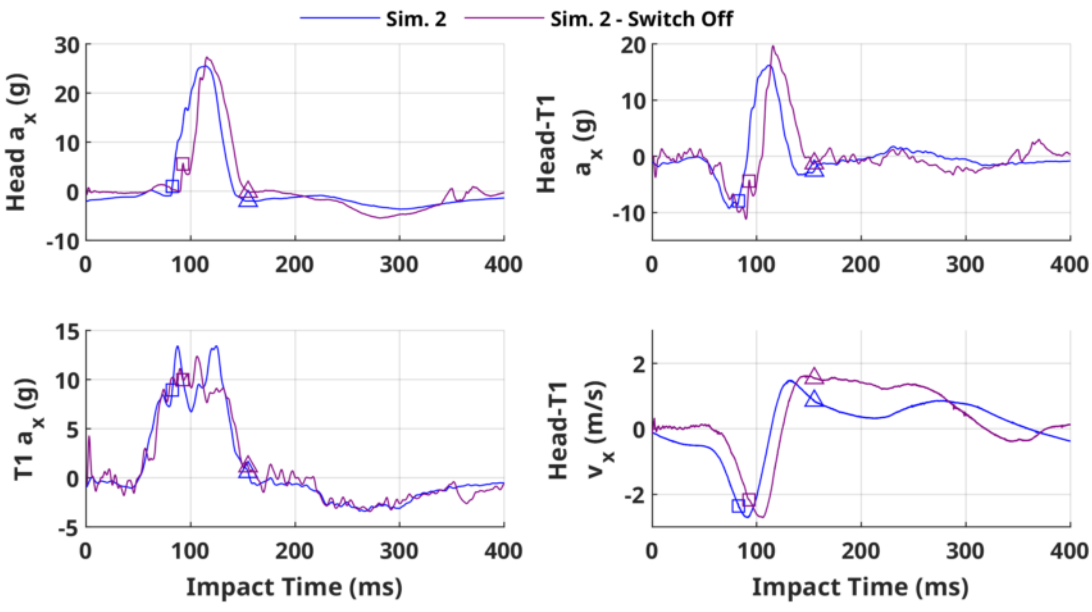

Fig. E2. The HBM head–T1 rear-end impact kinematics in Sim. 2 and the repeated Sim. 2 with muscle activations turned off at the start of impact. The square marker indicates the head-to-head restraint contact time, and the triangle timing of rebound when the head left the head-restraint.

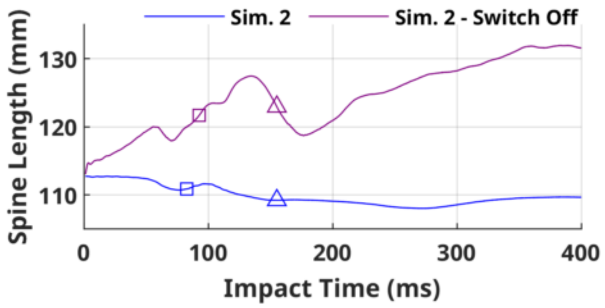

Fig. E3. The HBM cervical spine length during the rear-end impact for Sim. 2 and the repeated Sim. 2 with muscle activations turned off at the start of impact, calculated as the Euclidean distance between the C1–T1 vertebra markers (see also Fig. 3). The square marker indicates the head-to-head restraint contact time, and the triangle timing of rebound when the head left the head-restraint.

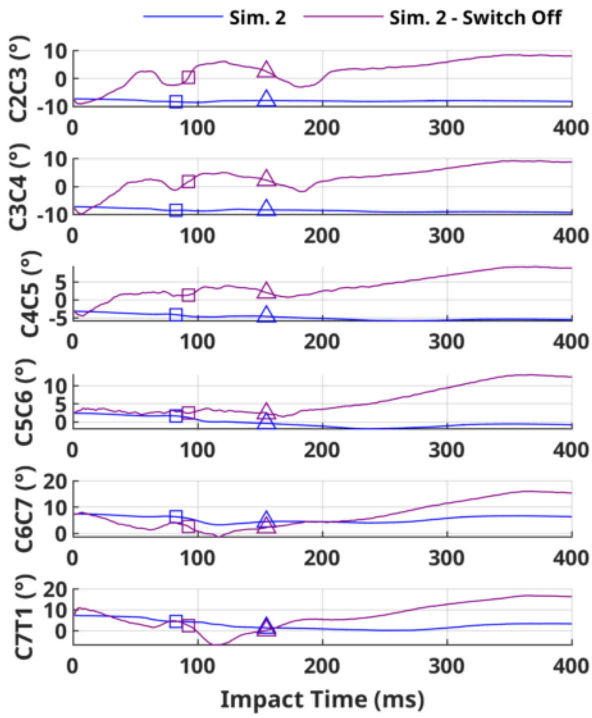

Fig. E4. The HBM cervical spine segment rotations during the rear-end impact in Sim. 2 the repeated Sim. 2 with muscle activations turned off at the start of impact. The square marker indicates the head-to-head restraint contact time, and the triangle timing of rebound when the head left the head-restraint.